Parallel Entanglement Distribution on Hypercube Networks

BY
Christopher Chudzicki
WITH
Frederick W. Strauch, Advisor

A thesis submitted in partial fulfillment
of the requirements for the
Degree of Bachelor of Arts with Honors
in Physics

WILLIAMS COLLEGE
Williamstown, Massachusetts

August 6, 2010

Contents

Acknowledgements

I owe a great deal to many people who have aided in the production of this thesis, and I am grateful to all who have contributed. First, I would like to thank my parents, who have supported me in all of my pursuits, and have especially encouraged my love of science. My mother was in fact my first quantum mechanics instructor.

Secondly, I wish to thank all of the others who have taught me physics, but especially my high-school physics teachers Steven Cotts and Christopher Shanks, and two members of the Williams College Physics Department: Ward Lopes, for his aid as second reader, and Bill Wootters from whom I learned to love theoretical physics and quantum information theory in particular.

Most importantly, I wish to thank my thesis advisor Professor Frederick Strauch, to whom I am deeply indebted. He has taught me many things. I have truly enjoyed learning about quantum computation and quantum state transfer from him for the last year. Perhaps most importantly, though, he has a practical bent that I can only hope has rubbed off on me. Without his guidance and support, my research and this thesis would not have been possible.

Executive Summary

A quantum computer, a computer based upon the manipulation of quantum systems, could solve many problems considered difficult for conventional computers. However, a quantum computer large enough to be useful would likely need to contain many distinct registers. Before such a quantum computer can be built, it must be possible to efficiently route quantum information (quantum states) from one register of the quantum computer to another, just as classical information is routed in a conventional computer. In this work we study the efficiency and faithfulness of *parallel* entanglement transfer on quantum networks. Once transferred, entanglement can be distilled and used to teleport arbitrary quantum states.

By "quantum network" we mean a network of coupled quantum systems, and in particular, either spin-$\frac{1}{2}$ particles, also known as quantum bits (qubits), or simple harmonic oscillators. Such a network is conveniently visualized as a graph, as in Figure 1 for the cube. We consider the following situation. At each node of this network there is a register of the quantum computer (a collection of qubits) and each register is capable of generating pairs of qubits in the Bell state $|\Phi^+\rangle = (|0\rangle|0\rangle + |1\rangle|1\rangle)/\sqrt{2}$. Some subset of the nodes $\{s_1 \dots s_M\}$ act as senders, and some subset $\{r_1 \dots r_M\}$ act as receivers. The goal of sender s_j is to faithfully transfer half of her entangled pair to receiver r_j, so that these two nodes can then communicate via teleportation. The senders and receivers use the following protocol to attempt to transfer entanglement.

Parallel Entanglement Transfer on a Quantum Network by Dynamical Evolution

Step 1: Each sender s_j is in possession of a qubit-node pair in a Bell state $|\Phi^+\rangle$. Every node (oscillator or qubit) not associated with a sender is in the state $|0\rangle$.

Step 2: The quantum network is allowed to evolve according the the natural time evolution of its Hamiltonian for some time T (the transfer time). Each sender's qubit is kept isolated, so that it does not evolve in time.

Step 3: Each receiver r_j transfers the state of his node to a qubit in his possession.

Step 4: The sender and receiver each perform predetermined local operations on their qubits. The state of the qubit pair is now denoted by $\widetilde{\rho}_j(T)$.

The faithfulness of the entanglement transfer from sender s_j to receiver r_j is quantified by the fidelity

$$F_{s_j \to r_j}(T) = \langle \Phi^+ | \widetilde{\rho}_j(T) | \Phi^+ \rangle. \tag{1}$$

The fidelity of the transfer ranges from 0 to 1, with $F_{s_j \to r_j}(T) = 1$ indicating that perfect transfer has been achieved in a time T. The transfer time T is chosen so as to maximize the fidelity.

Quantum state transfer and entanglement transfer *for a single user* via this and other protocols on spin networks has been well-studied in the literature [1]. It would, of course, be much more efficient if multiple nodes could faithfully send entanglement through the network *at the same time*—in other words, if multiple senders could use the quantum network in parallel. It is the goal of this thesis to, for the first time, study the new errors that arise from such parallel quantum entanglement transfer.

The general Hamiltonian $\mathcal{H}$ that we consider for an oscillator network with network graph $\mathcal{G} = (V, E)$ is

$$\mathcal{H} = \hbar \sum_{v \in V} \Omega_{vv} a_v^\dagger a_v + \hbar \Omega_0 \sum_{\{u,v\} \in E} \left(a_u^\dagger a_v + a_v^\dagger a_u \right). \tag{2}$$

where $a_v^\dagger$ and a_v are the creation and annihilation operators for the oscillator at vertex v. The corresponding spin-network Hamiltonian that we consider is

$$\mathcal{H} = -\frac{1}{2}\hbar \sum_{v \in V} \Omega_{vv} \sigma_z^{(v)} + \frac{1}{2}\hbar \Omega_0 \sum_{\{u,v\} \in E} \left(\sigma_x^{(u)} \sigma_x^{(v)} + \sigma_y^{(u)} \sigma_y^{(v)} \right), \tag{3}$$

where $\sigma_x^{(v)}$, $\sigma_y^{(v)}$, and $\sigma_z^{(v)}$ are the Pauli spin operators for the qubit at vertex v. While our results hold for any network of qubits coupled by an XY interaction, our research is inspired especially by networks of superconducting quantum bits.

We limit our attention to the case when the couplings between nodes are all equal, although we do allow that the on-site energies be programmable. By "programmable", we have in mind that the users of the quantum network have complete control over the on-site energies *and* that they can be changed quickly, from one use of the network to another (but not during any given use of the network). Programmable qubits in this sense have been synthesized, [2, 3, 4], but to our knowledge dynamically tunable couplings have not been demonstrated.

It is well known that a single user can transfer entanglement from corner-to-corner of a d-dimensional hypercube in constant time $T = \frac{\pi}{2\Omega_0}$ [5], depicted in Figure 1(a). In this sense a d-dimensional hypercube is a great channel of quantum information between antipodal nodes. A d-dimensional hypercube can be broken up into 2^m subcubes of dimension $d - m$. These subcubes can be made to act as good channels between *their* antipodal nodes by detuning the on-site energies for the entire channel from the on-site energies from adjacent channels, shown in Figures 1(b) and 1(c) for a $d = 3$ oscillator network.

A main result of this thesis, derived in Chapter 2, is that it is possible to split a d-dimensional hypercube oscillator network into 2^m subcube channels, and that one sender-receiver pair can use each subcube channel to transfer entanglement with fidelity F bounded from below by

$$F \gtrsim 1 - \frac{3}{2} m \, \eta^2 \sin^2 \xi_T, \tag{4}$$

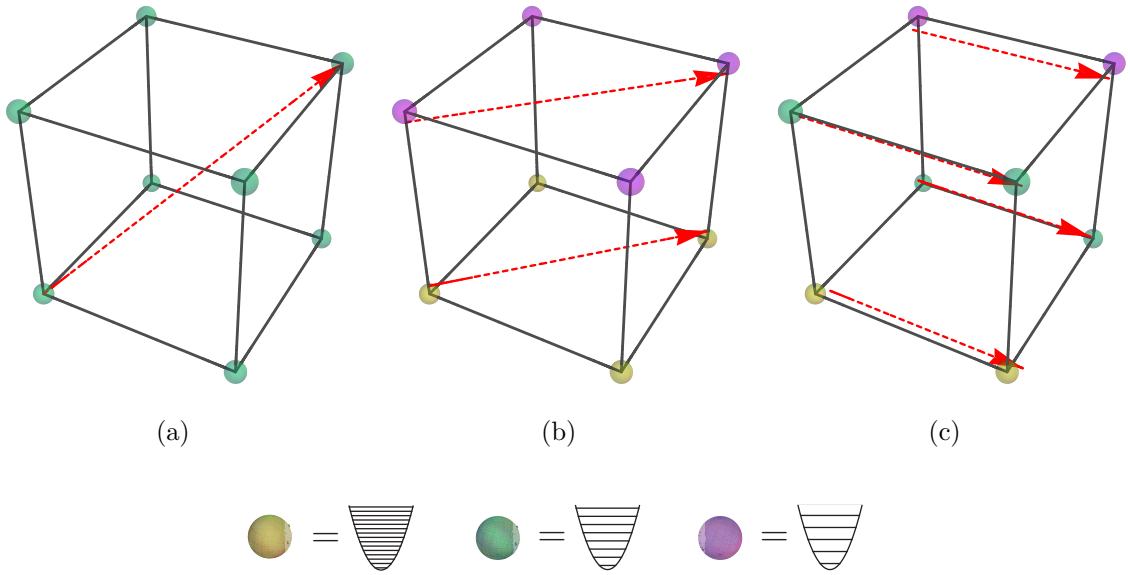

Figure 1: Arrows denote the transfer of entanglement. **(a):** Perfect state transfer is possible from corner to corner of a symmetric d-dimensional hypercube. **(b):** A 3-cube can be split up into two effectively decoupled 2-cube channels (opposing faces). **(c):** A 3-cube can also be split into four effectively decoupled 1-cube channels (pairs).

where $\eta = \frac{2\Omega_0}{\Delta\omega}$, $\xi_T = \sqrt{1+\eta^{-2}}$, and $\Delta\omega$ is the detuning between adjacent channels. Here "$\gtrsim$" means that this lower bound is correct to second order in η. If $\eta \ll 1$, then each sender transfers entanglement to her corresponding receiver with high fidelity. Notice that the error in the fidelity is proportional to $\sin^2 \xi_T$—by picking η just right, one can make $\sin^2 \xi_T$, the error term, vanish. The fidelity thus exhibits resonances. We stress that, for oscillators, when the fidelity is on resonance it is truly perfect (to all orders in η).

Equation (4) was derived as a lower bound for entanglement transfer on oscillator networks. However, as long as only one sender-receiver pair uses each channel at a time, as in Figure 1, there is numerical evidence to suggest that qubit networks behave similarly. For this reason we call the parallel state transfer protocol discussed so far the "qubit-compatible" (QC) protocol. Figure 2 compares the fidelity of entanglement transfer on hypercubes of spins to a lower bound on the corresponding fidelity for hypercubes of oscillators. The behaviors are qualitatively similar, with a few important differences. Most notably, qubits do better on average, but cannot achieve perfect state transfer. Also, for oscillators the fidelity of the entanglement transfer is independent of the dimension of the hypercube network d (depending only on the number of channels 2^m into which it is split); for qubits, though, there is some d dependence when η is not small.

Besides the ability to perform truly perfect parallel state transfer, oscillator networks have another, highly desirable feature that qubit networks lack: the capacity for massively-parallel (MP) entanglement transfer. Because excitations on an oscillator

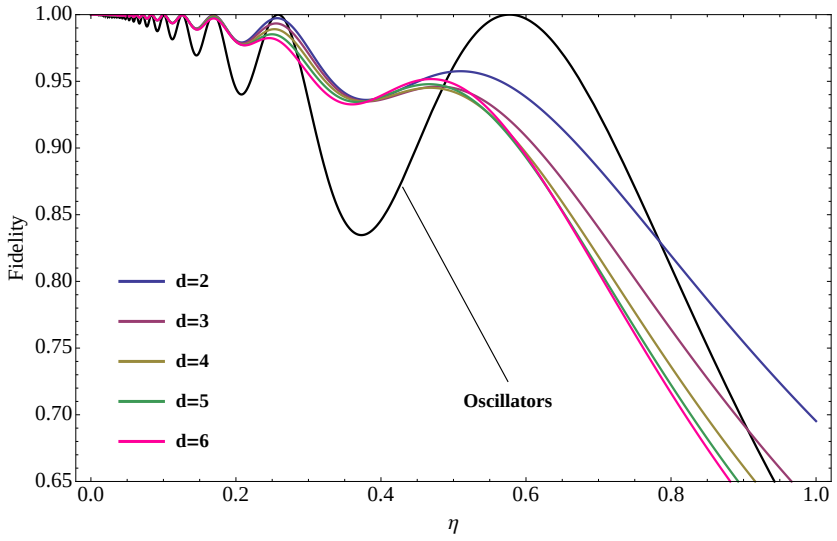

Figure 2: The fidelity of entanglement transfer for a d-dimensional hypercube network of spins split into two channels with one sender and receiver per channel, with entanglement being sent in the same direction on each channel for $d = 2$ through 6. Shown also is an exact lower bound on the entanglement fidelity for transfer via a hypercube oscillator network split into two subcube channels in the same manner; the oscillator fidelity is the same for all dimensional hypercubes.

network pass through each other without interacting, *every* node on an oscillator hypercube network can act as a sender at once without decreasing the fidelity bounded by (4).

Parallel entanglement transfer is thus theoretically possible. In Chapter 3, we ask: how much more efficient is it than single-user (serial) protocols? Suppose that at each node of the quantum network there is a register of the quantum computer, and that the goal is for each pair of registers to share a large number of Bell states. We define the distribution time T_D as the time it takes for each pair of nodes to share an approximate Bell pair, and the rate as the number of pairs shared, weighted by their fidelities, divided by the distribution time:

$$\mathcal{R} = \frac{1}{T_D} \sum_{\text{pairs } \{u,v\}} F_{u \to v}. \tag{5}$$

We show that for a hypercube with $N = 2^d$ nodes, the rates of the qubit-compatible (QC) protocol and the massively-parallel protocol (MP) are bounded from below by

$$\mathcal{R}^{(\text{QC})} \gtrsim \frac{1}{T} N^{0.415} \left(1 - \frac{3}{4} \left(\frac{\Omega_0}{\omega_{\max} - \omega_{\min}} \right)^2 d^2(d+3) \right), \tag{6}$$

$$\mathcal{R}^{(\text{MP})} \gtrsim \frac{1}{T} N \left(1 - \frac{3}{4} \left(\frac{\Omega_0}{\omega_{\max} - \omega_{\min}} \right)^2 d^2(d+3) \right), \tag{7}$$

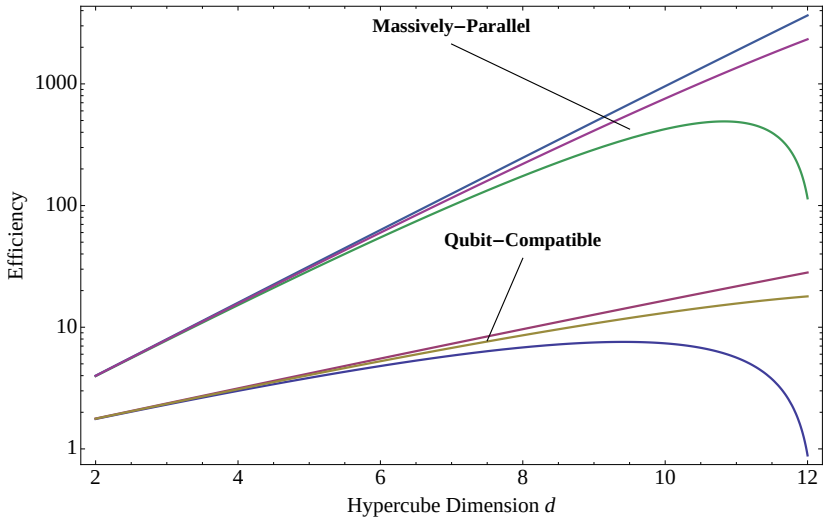

Figure 3: A comparison of the qubit-compatible and massively-parallel entanglement distribution rates on hypercube networks with $\frac{2\Omega_0}{\omega_{\max}-\omega_{\min}} = 0.01, 0.02, 0.03$.

where $\omega_{\max} - \omega_{\min}$ is the bandwidth within which all the on-site energies must lie. The rate of any serial protocol is bounded from below by unity, so both parallel protocols do better, even for modest network sizes, as long as $\frac{\Omega_0}{\omega_{\max}-\omega_{\min}} \ll 1$. We stress that (6) and (7) are lower bounds on the rates: if the senders fully utilize the resonances exhibited in the fidelity, it may be possible to achieve better rates even for small bandwidths $\omega_{\max} - \omega_{\min}$.

The bounds (6) and (7) are plotted as a function of $d = \log_2 N$ for various bandwidths in Figure 3. The massively-parallel protocol is more than quadratically better, though there are significant technical challenges to any transfer protocol that relies on oscillators. Most notably, such methods require an interface between the qubit register and the network itself. Still, such an interface has been recently achieved in the laboratory [6].

We show, then, that high-fidelity parallel entanglement transfer is achievable on hypercube quantum networks with equal couplings and programmable on-site energies. Considering two entanglement distribution schemes on oscillator networks, qubit-compatiable and massively-parallel distribution, we show that both of these offer a speedup over the serial protocols, but that the oscillator-dependent, massively-parallel scheme is vastly more efficient.

Chapter 1

Introduction

A large-scale quantum computer, if realized, would outperform classical computers on certain key problems. Most famously, Shor's algorithm, if implemented, would allow a quantum computer to rapidly factor large numbers and thereby defeat many current cryptosystems [7]. Quantum computers are usually envisioned as collections of qubits—quantum bits, or generic two-state quantum systems—on which arbitrary unitary transformations can be performed. In other words, a quantum computer is a quantum system over which the operator has complete control.

A quantum computer large enough to be useful would probably need to contain several distinct registers of qubits. In order to perform arbitrary operations on the qubits, it would be necessary to route quantum information (i.e. the states of qubits) from one register to another. Because of the (hopefully) short physical distances between registers, photons, while ideal for long-range communication (quantum or otherwise), would be an inconvenient way to transmit quantum information in quantum computers. The use of photons for communication would also require a special interface to transfer the state of a qubit (perhaps a spin-$\frac{1}{2}$ particle or an element of a superconducting quantum circuit) to a photon. These difficulties have inspired many researchers to look for alternative, non-photonic methods of quantum information routing.

In this thesis we study two alternatives to quantum communication via photons: spin networks and oscillator networks, with an emphasis on hypercube architectures. While most of our analytic results are specific to oscillator networks, we argue that many of our findings are qualitatively similar to the (harder to compute) corresponding results for spin networks. In Chapter 1 we review some basics of single-state quantum transfer. In Chapters 2 and 3 we present original research on parallel quantum state transfer.

1.1 Spin Chains

One attractive alternative to photonic quantum communication is to transfer quantum states using a "wire" of qubits, as in Figure 1.1. A qubit, or quantum bit, is any two-state quantum system whose levels are usually labelled by $|0\rangle$ and $|1\rangle$. For

ease of exposition, and because chains of coupled spin-$\frac{1}{2}$ particles are well-studied in the condensed matter literature, such wires are often referred to as spin chains. Spin chains are an appealing possibility for quantum state transfer inside quantum computers because the chain could be made out of the same type of qubits as the registers, eliminating (or at least reducing) the need for any interface between the information channel and the register.

In the absence of external magnetic fields, the Hamiltonian for a length N spin chain with nearest-neighbor XY interactions is

$$\mathcal{H} = \frac{1}{2}\hbar \sum_{j=1}^{N-1} \Omega_{jj+1} \left(\sigma_x^{(j)} \sigma_x^{(j+1)} + \sigma_y^{(j)} \sigma_y^{(j+1)} \right), \tag{1.1}$$

where $\sigma_x^{(j)}$ and $\sigma_y^{(j)}$ (along with $\sigma_z^{(j)}$) are the usual Pauli spin operators[1] for qubit j, and Ω_j is the strength of the coupling between spins j and $j+1$. The ground state of this Hamiltonian has every qubit in the state $|0\rangle$. There are, of course, other possible couplings. One alternative, the Heisenberg model, has couplings of the form $\vec{\boldsymbol{\sigma}}^{(j)} \cdot \vec{\boldsymbol{\sigma}}^{(j+1)}$ where $\vec{\boldsymbol{\sigma}}^{(j)} = (\sigma_x^{(j)}, \sigma_y^{(j)}, \sigma_z^{(j)})$. In this work, however, we focus exclusively on XY coupling interaction, as this is the type of coupling that arises in superconducting qubits [8].

Now suppose that there is a sender s at one end of the spin-chain who is in possession of an arbitrary, possibly unknown qubit state $|\psi\rangle = \alpha|0\rangle + \beta|1\rangle$ that she wishes to transfer to a receiver, r, at the other end of the chain. Because the state $|\psi\rangle$ is potentially unknown, the sender cannot simply use classical communcation to tell the receiver to prepare a qubit in the state $|\psi\rangle$. Similarly, a single measurement on a quantum state reveals only partial information, and since arbitrary quantum states cannot be cloned [9], she is prevented from determining her qubit's state.

The sender could, however, attempt to use the spin-chain to transfer the state $|\psi\rangle$ over to the receiver. One scheme that the sender and receiver might try is as follows.

Spin Chain State Transfer Protocol

Step 1: Initialize the transfer by preparing each spin in the state $|0\rangle$, except prepare the sender's spin in the state $|\psi\rangle$ (Figure 1.1(a)).

Step 2: Wait for some time T (the transfer time), letting the chain evolve naturally according to its Hamiltonian.

Step 3: The receiver removes his qubit from the spin chain, and performs some predetermined *local* unitary operation U on his qubit.

The transfer is said to be perfect if, after Step 3, the receiver possesses a qubit in exactly the state $|\psi\rangle$ (Figure 1.1(b)); the transfer is considered successful if the receiver's qubit is in a state close to $|\psi\rangle$ (this will be made rigorous shortly). It is also desirable that the transfer time T be short. The receiver is allowed to perform

[1] Our convention is that $|0\rangle$ is the $+1$ eigenstate of σ_z, and $|1\rangle$ is the -1 eigenstate of σ_z.

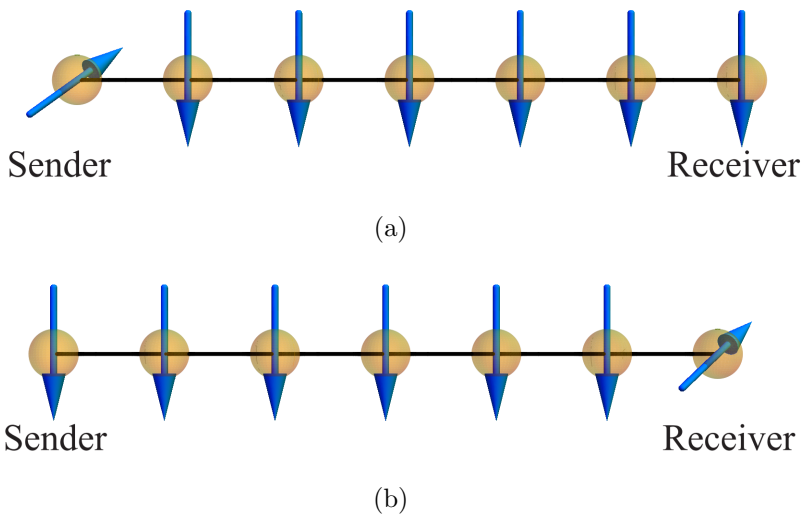

Figure 1.1: **(a):** The initialized spin chain. **(b):** The ideal state of the chain at the transfer time T, in which the sender's qubit state has faithfully travelled to the receiver.

a predetermined local unitary operation on his qubit at the end of the protocol to undo some of the effects of the spin chain on $|\psi\rangle$. For example, it may be known that as a state traverses the chain it merely picks up a constant relative phase $e^{i\varphi}$. The receiver's spin before he operates with any unitary would then be in the state $\alpha|0\rangle + e^{i\varphi}\beta|1\rangle$. In this case the unitary would be chosen so as to undo that relative phase shift.

Spin chains have been well-studied in the literature. It is, for example, known that perfect state transfer is impossible on a chain of length $N \geq 4$ if the couplings Ω_j are all equal, but if the couplings are tunable and allowed to be arbitrarily large, then perfect state transfer can be achieved on a spin chain of arbitrary length in constant time [5]. It is also important to note that there are many generalizations and variations of the protocol described above. First, one can replace a spin chain by a more general network of spins, to be described in the following section. Second, the qubits (two-level quantum systems) can be replaced by qudits (d-level quantum systems), or even oscillators. In Chapter 2 we will consider such oscillator networks. Third, one can modify the state initialization step to prepare the non-sender spins in another initial state, which could even be a mixed state (e.g. a thermal state). It is, of course, necessary that the sender's spin begins in the state $|\psi\rangle$ that she wishes to transfer[2]. We will use such a modification in Chapter 2. Finally, while we will focus on transfer through natural dynamical evolution in this thesis, there are other schemes which incorporate measurements [10] to achieve perfect state transfer. These and other generalizations are reviewed by Bose [1]

[2]This is a bit of an overstatement. If the sender wishes to transfer the state $|\psi\rangle$, it's fine if her spin is in the state $|\phi\rangle$, as long as she knows how $|\psi\rangle$ and $|\phi\rangle$ are related, and can tell the receiver—but let's assume that her spin must be in the state $|\psi\rangle$.

1.2 Spin Networks

As a generalization of spin chains, we consider the situation in which the sender and receiver are connected by a network of coupled spins with arbitrary geometry. We will see that perfect quantum state transfer can be achieved on certain arbitrarily large networks whose couplings are equal [5]. Such a network is conveniently visualized as a graph, as in Figure 1.2.

A *graph* $\mathcal{G} = (V, E)$ is a set V of vertices (or nodes) together with an edge set E. One of the vertices $s \in V$ is the sender vertex, one vertex $r \in V$ is the receiver vertex. The elements of the edge set are two-element subsets of V. If $u, v \in V$ are vertices of the graph, we say that u is connected[3] to v if $\{u, v\} \in E$. The order of a graph is $|V|$, the number of vertices. A convenient representation of the graph $\mathcal{G}$, which is extraordinarily important in the study of spin networks, is its *adjacency matrix* A. An element A_{uv} of the adjacency matrix is 1 if $\{u, v\} \in E$, and zero otherwise. The adjacency matrix is real and symmetric.

Graphs are often used to study information routing in classical computers. Nodes connected by edges can represent individual registers connected by classical communication channels. Finding a network that can efficiently route information between all nodes is a well-studied problem in computer science. The corresponding problem in quantum information science is to find a network of coupled quantum systems (such as qubits) in which quantum information can be efficiently routed.

Given a graph $\mathcal{G} = (V, E)$ of order N one can define corresponding Hamiltonians by

$$\mathcal{H} = \frac{1}{2}\hbar \sum_{\{u,v\}\in E} \Omega_{uv} \left(\sigma_x^{(u)}\sigma_x^{(v)} + \sigma_y^{(u)}\sigma_y^{(v)}\right). \tag{1.2}$$

Of particular interest are Hamiltonians in which the couplings Ω_{u-v} are all equal, because such systems are easier to manufacture in practice [1]. We shall focus exclusively on such spin networks. We will, however, allow for a programmable energy difference $\hbar\Omega_{vv}$ (the "on-site" energy) between the two qubit states (if the qubits are literal spins, this could be achieved with local, tunable magnetic fields). In this case, the oscillator networks corresponding to $\mathcal{G}$ has a Hamiltonian of the form,

$$\mathcal{H} = -\frac{1}{2}\hbar \sum_{v\in V} \Omega_{vv}\sigma_z^{(v)} + \frac{1}{2}\hbar\Omega_0 \sum_{\{u,v\}\in E} \left(\sigma_x^{(u)}\sigma_x^{(v)} + \sigma_y^{(u)}\sigma_y^{(v)}\right) + V_0\mathcal{I}, \tag{1.3}$$

where $\mathcal{I}$ is the identity operator on the state-space of the spins, and V_0 is some constant. In saying that the Ω_{vv}'s are programmable, we have in mind that the operators of the spin network can choose the Ω_{vv}'s to be whatever they like, *and* that they can be changed from one use of the network to another. Programmable

[3]Sets are inherently unordered, so if u is connected to v, then v is connected to u. Graphs as defined here are sometimes called *undirected* graphs; if the edge set is a set of order pairs (instead of subsets) of V, the graph is called *directed*. Also, we've specified that the edge set is a set of *two*-element subsets of V, and so no edges connect a node to itself—in other words, our graphs are *simple*.

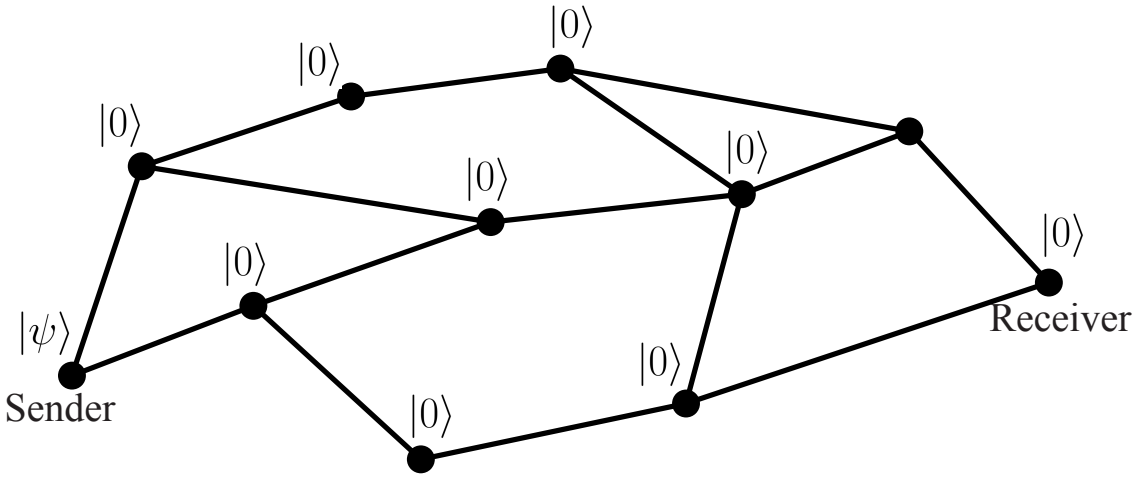

Figure 1.2: An initialized spin network. Note that, although each non-sender qubit starts in the state $|0\rangle$ in this figure, this is not necessary.

qubits in this sense have been demonstrated [11, 6, 2, 3, 4], but to our knowledge programmable couplings have not.

The state $|\text{vac}\rangle = |00\ldots00\rangle$, in which every qubit is in the state $|0\rangle$, is an eigenstate of (1.3) (it's name, $|\text{vac}\rangle$, is inspired by the vacuum state of quantum field theory). Without loss of generality, we can assume that V_0 is chosen so that $|\text{vac}\rangle$ has zero energy, and that the Ω_{vv}'s are always chosen so that $|\text{vac}\rangle$ is the ground state of the Hamiltonian (1.3).

The general protocol for using a spin network to transfer quantum states via dynamical evolution is the same as the protocol described in Section 1.1 for spin chains. However, we again stress that the non-sender qubits need not start in the $|0\rangle$ state, although this is the situation depicted in Figure 1.2.

How faithfully does a spin network transfer quantum states between the sender and receiver (when used with a particular protocol)? Suppose that a sender, wishing to transfer a qubit state $|\psi\rangle$ to some receiver, initializes the quantum network. We denote the quantum state of the entire network at time t by $|\text{network}(t)\rangle$, and take $t = 0$ at initialization. At time t, the receiver's qubit may not have a state vector of its own—it may be in a mixed state, *entangled* with the other network qubits. Entanglement will be discussed further in Section 1.3, but this essentially means that the results of measurements on the receiver's qubit could be correlated with the results of measurements on other qubits. The proper way to describe such a state is via its *reduced density matrix* $\rho_R(t)$. To calculate the reduced density matrix $\rho_R(t)$ for the receiver's qubit, one imagines that some observer measures every other component of the spin network, but doesn't tell us the answer. Because we don't know the measurement results, we must average over all possible outcomes. Mathematically,

this is achieved by

$$\rho_R(t) = \mathrm{Tr}_{v\neq r}|\mathrm{network}(t)\rangle\langle\mathrm{network}(t)|, \tag{1.4}$$

where $\mathrm{Tr}_{v\neq r}$ denotes a partial trace over all qubits except the receiver's qubit. For more on the reduced density matrix, see [7].

At the transfer time T, the receiver removes his qubit from the network and then performs some predetermined unitary operation on his qubit. The state of his qubit after he performs this operation is

$$\widetilde{\rho}_R(T) = U^\dagger \rho_R(T) U. \tag{1.5}$$

The faithfulness of the state transfer from the sender (at vertex s) to the receiver (at vertex r) is quantified by the *fidelity*, $F_{s\to r}$, of the state $\widetilde{\rho}_R(T)$ with the state $|\psi\rangle$ that the sender was trying to transfer:

$$F_{s\to r}(T) = \langle\psi|\widetilde{\rho}_R(T)|\psi\rangle. \tag{1.6}$$

The fidelity has the following simple interpretation: if someone makes a projective measurement on the receiver's qubit, asking whether it is in the state $|\psi\rangle$ or not, the fidelity is the probability of a positive result. For more on fidelity as a distance measure between quantum states, see [7]. The transfer time T and the receiver's unitary U are picked so as to maximize the fidelity; the state transfer is said to be perfect if $F(T) = 1$. Again, the receiver's unitary U is predetermined: it cannot depend on the state $|\psi\rangle$ being sent, which is generally unknown. A common way to characterize the quality of a network is to a calculate the fidelity averaged over all possible input states.

1.2.1 Time Evolution and the Graph Space

Because the spin network Hamiltonian (1.3) is time-independent, the time evolution operator $\mathcal{U}_t$ is given by

$$\mathcal{U}_t = e^{-i\mathcal{H}t/\hbar}. \tag{1.7}$$

Now, consider the total number operator $N^{(\mathrm{tot})} = \sum_v \frac{I-\sigma_z^{(v)}}{2}$, which just counts the number of qubits in the $|1\rangle$ state. The state-space of the spin network splits up into subspaces corresponding to different eigenvalues of $N^{(\mathrm{tot})}$. The eigenvalues for an N-node network are $0, 1, \ldots, 2^N$. The eigenspace corresponding to eigenvalue ℓ has dimension $\binom{2^N}{\ell}$, and consists of all the states which have ℓ nodes in the $|1\rangle$ state and the rest in the $|0\rangle$ state.

The total number operator $N^{(\mathrm{tot})}$ commutes with the Hamiltonian—in fact, it commutes with each term[4] of the Hamiltonian. The identity commutes with everything, so we need only check that $S_z^{(\mathrm{tot})} = \sum_v \sigma_z^{(v)}$ commutes with each term. Since

[4]The fact that $[\mathcal{H}, N^{(\mathrm{tot})}] = 0$ is thus true even if the couplings Ω_{uv} are not all equal.

Pauli operators for different qubits commute we need not worry about the coupling term:

$$\begin{aligned}\left[\sigma_x^{(u)}\sigma_x^{v}+\sigma_y^{(u)}\sigma_y^{(v)}, S_z^{(\mathrm{tot})}\right] &= \left[\sigma_x^{(u)}\sigma_x^{v}, \sum_w \sigma_z^{(w)}\right] + \left[\sigma_y^{(u)}\sigma_y^{(v)}, \sum_w \sigma_z^{(w)}\right] \\ &= [\sigma_x^{(u)}, \sigma_z^{(u)}]\sigma_x^{(v)} + [\sigma_y^{(u)}, \sigma_z^{(u)}]\sigma_y^{(v)} + \sigma_x^{(u)}[\sigma_x^{(v)}, \sigma_z^{(v)}] + \sigma_y^{(u)}[\sigma_y^{(v)}, \sigma_z^{(v)}] \\ &= i\left(-\sigma_y^{(u)}\sigma_x^{(v)} + \sigma_x^{(u)}\sigma_y^{(v)} - \sigma_x^{(u)}\sigma_y^{(v)} + \sigma_y^{(u)}\sigma_x^{(v)}\right) = 0. \qquad (1.8)\end{aligned}$$

The total number of excitations, then, is conserved. The time evolution operator $\mathcal{U}_t$ maps states in the ℓ-excitation subspace to states within the ℓ-excitation subspace. In other words, the Hamiltonian $\mathcal{H}$ of (1.3) and the time evolution operator $\mathcal{U}_t$ are block-diagonal: the dynamics of the ℓ-excitation subspace is determined completely by the ℓ-excitation block of $\mathcal{H}$ (and, more directly, $\mathcal{U}_t$).

In particular, the off-diagonal portion of the single-excitation block of the Hamiltonian is proportional to the adjacency matrix A of the network graph and its diagonal elements are just the on-site energies $\hbar\Omega_{vv}$. Before showing this, we clarify a bit of terminology and notation.

Associated with the order-N graph $\mathcal{G} = (V, E)$ is an N-dimensional vector space, the graph-space. For each vertex $v \in V$ there is a corresponding basis vector $|v\rangle_{\mathcal{G}}$ of the graph-space. We will use Dirac notation for vectors in both the graph-space and the state-space of the quantum network, but graph-space kets will receive a subscript $\mathcal{G}$ to distinguish them from vectors in the much larger, 2^N-dimensional state-space[5]. Expressed in this notation, the adjacency matrix, an operator on graph-space, has matrix elements

$$\langle u|A|v\rangle_{\mathcal{G}} = \begin{cases} 1 & \text{if } \{u, v\} \in E \\ 0 & \text{otherwise} \end{cases} \qquad (1.9)$$

There is a natural correspondence between the basis vector $|v\rangle_{\mathcal{G}}$ for a node in the graph-space and the quantum state $|v\rangle = \sigma_x^{(v)}|\mathrm{vac}\rangle$ which has every qubit in the state $|0\rangle$, except the qubit at vertex v which is in the state $|1\rangle$.

To prove the claim made above about the form of the single-excitation block of the spin network's Hamiltonian, one calculates that $\langle u|\sigma_x^{(u')}\sigma_x^{(v')}+\sigma_y^{(u')}\sigma_y^{(v')}|v\rangle = 2\delta_{u,u'}\delta_{vv'}$. Then, since the constant V_0 is chosen so that $|\mathrm{vac}\rangle$ is the zero-energy state, we have

$$\langle u|\mathcal{H}|v\rangle = \hbar\Omega_{vv}\delta_{uv} + \hbar\Omega_0\langle u|A|v\rangle_{\mathcal{G}}.$$

The adjacency matrix of the network graph thus largely determines the dynamics of the single excitation subspace: the single-excitation block of the Hamiltonian is $\hbar\Omega$, where Ω is an $N \times N$ matrix whose elements $\langle u|\Omega|v\rangle$ are the coefficients Ω_{uv} that appear in the definition (1.3) of the Hamiltonian. The time evolution of the state $|v\rangle$ can be written explicitly in terms of Ω:

$$\mathcal{U}_t|v\rangle = \sum_u \langle u|\mathcal{U}_t|v\rangle|u\rangle = \sum_u \langle u|e^{-i\Omega t}|v\rangle_{\mathcal{G}}|u\rangle. \qquad (1.10)$$

[5]Graph space bras receiver no subscript; it should be clear from context that they are in the graph space. Thus, the matrix element in (1.9) is written as $\langle u|A|v\rangle_{\mathcal{G}}$, not ${}_{\mathcal{G}}\langle u|A|v\rangle_{\mathcal{G}}$.

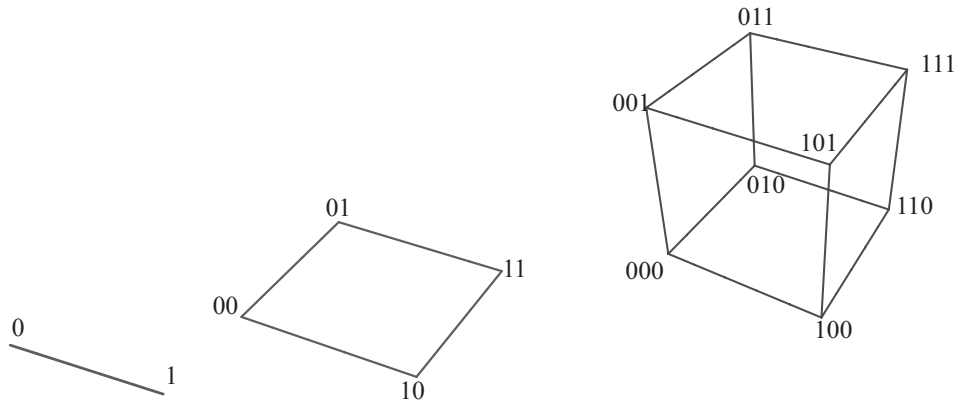

(a) d=1 (b) d=2 (c) d=3

Figure 1.3: Hypercubes of dimension 1-3.

1.2.2 Perfect State Transfer: Hypercube Networks

Hypercube networks have a rich history. Among the earliest studied networks in computer science [12, 13], hypercube networks are appealing from a theoretical viewpoint because they are highly symmetric and possess a hierarchical structure. On the practical side, hypercubes also offer an efficient way to connect a large number of vertices: connecting the N vertices of a hypercube requires only $N \log_2 N^{1/2}$ edges. For this reason, the builders of the Connection Machine, an early, massively-parallel supercomputer constructed in the 1980's (and famous as a favorite summer project of Feynman's) chose to connect the computer's processors with a hypercube geometry [14]. It is only natural to study the quantum mechanical properties of network with so high a pedigree.

The hypercube graph of dimension d is defined as follows. Each element of the vertex set V is a bitstring of length d,

$$V = \{\mathbf{z} | \mathbf{z} = z_d \dots z_1,\ z_j \in \{0, 1\}\} = \mathbb{Z}_2^d. \tag{1.11}$$

The *Hamming distance* $d_H(\mathbf{z}, \mathbf{z}')$ is defined as the number of bits in which $\mathbf{z}$ and $\mathbf{z}'$ differ. A pair of vertices $\{\mathbf{z}, \mathbf{z}'\}$ is in the edge set E if and only if the Hamming distance between them is exactly 1. The first three hypercubes are shown in Figure 1.3.

To calculate the dynamics of the single-excitation subspace of a d-dimensional hypercube quantum spin network, we utilize the tensor product structure of the hypercube graph-space [5]. The vector $|\mathbf{z}\rangle_{\mathcal{G}}$ associated with vertex $\mathbf{z}$ can be written as a d-fold tensor product of the two-dimensional vectors $|0\rangle = \left(\begin{smallmatrix}1\\0\end{smallmatrix}\right)$ and $|1\rangle = \left(\begin{smallmatrix}0\\1\end{smallmatrix}\right)$:

$$|\mathbf{z}\rangle_{\mathcal{G}} = (|z_d\rangle \otimes \cdots \otimes |z_1\rangle)_{\mathcal{G}} = |z_d \dots z_1\rangle_{\mathcal{G}}. \tag{1.12}$$

Because the elements $\langle \mathbf{z}|A|\mathbf{z}'\rangle$ are all either 0 or 1, and are nonzero if and only if the bitstrings $z_d \dots z_1$ and $z_d \dots z_1$ differ in exactly one place, the adjacency matrix is a

sum of tensor products of the 2×2 identity matrix I with the 2×2 Pauli matrix[6] $\sigma_x = \left(\begin{smallmatrix} 0 & 1 \\ 1 & 0 \end{smallmatrix}\right)$,

$$A = \sum_{j=1}^{d} X^{(j)}, \tag{1.13}$$

with

$$X^{(j)} = \left(\bigotimes_{k=j+1}^{d} \mathbb{I} \right) \otimes \sigma_x \otimes \left(\bigotimes_{k=1}^{j-1} \mathbb{I} \right). \tag{1.14}$$

The action of $X^{(j)}$ on $|\mathbf{z}\rangle$ is to flip the bit z_j: $X^{(j)}|z_d \dots z_j \dots z_1\rangle_{\mathcal{G}} = |z_d \dots \overline{z}_j \dots z_1\rangle_{\mathcal{G}}$, where $\overline{z}_j$ denotes the bit-flip of z_j.

We now consider the problem of quantum state transfer on a symmetric hypercube spin network—a hypercube network in which all of the on-site energies, $\hbar\Omega_{\mathbf{zz}}$ are equal (and, as always, the couplings are separately). Taking $\hbar\Omega_{\mathbf{zz}} = 0$ for definiteness, the Ω matrix is just $\Omega_0 A$. Suppose that the sender is at vertex $\mathbf{z}$ and the receiver at vertex $\overline{\mathbf{z}} = |\overline{z}_d \dots \overline{z}_1\rangle$, and that they initialize the network so each node's qubit is in the state $|0\rangle$, except the sender's qubit is in the state $|\psi\rangle = \alpha|0\rangle + \beta|1\rangle$ that she wishes to transfer. Using (1.10) for the evolution of single-excitation states, the quantum state of the network at time t is

$$|\text{network}(t)\rangle = \alpha|\text{vac}\rangle + \beta e^{-i\Omega_0 A t}|\mathbf{z}\rangle. \tag{1.15}$$

Because the adjacency matrix A is the sum of commuting matrices $X^{(j)}$, the matrix exponential of the sum is the product of the matrix exponentials:

$$e^{-i\Omega_0 A t} = e^{-i\Omega_0 t \sum_{j=1}^{d} X^{(j)}} = \prod_{j=1}^{d} e^{-i\Omega_0 t X^{(j)}}. \tag{1.16}$$

This can be evaluated using the identity $e^{-i(\hat{\mathbf{n}}\cdot\vec{\sigma})\phi} = \cos\phi - i(\hat{\mathbf{n}}\cdot\vec{\sigma})\sin\phi$. The result is

$$e^{-i\Omega_0 A t} = \prod_{j=1}^{d} \left(\cos(\Omega_0 t) I - i \sin(\Omega_0 t) X^{(j)} \right). \tag{1.17}$$

An immediate consequence is that at the time $T = \frac{\pi}{2\Omega_0}$ the quantum state of the network is

$$|\text{network}(T)\rangle = \alpha|\text{vac}\rangle + (-i)^d \beta|\overline{\mathbf{z}}\rangle. \tag{1.18}$$

The sender's state $|\psi\rangle$ has perfectly transferred to the receiver. The state $|\psi\rangle$ picked up a relative phase of $(-i)^d$, but this is no problem at all—the receiver can undo this relative phase shift by picking his unitary to be $U = \left(\begin{smallmatrix} 1 & 0 \\ 0 & i^d \end{smallmatrix}\right)$, independent of α and β.

[6] Our notation for Pauli matrices is as follows: σ_x is the 2×2 Pauli matrix; $\sigma_x^{(j)}$ is the Pauli operator on the state space of the quantum network; $X^{(j)}$ is the $2^d \times 2^d$ matrix operator on the graph space of the d-dimensional hypercube.

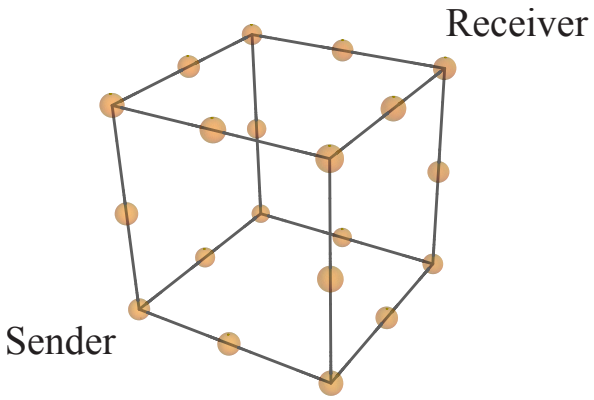

Figure 1.4: Perfect state transfer is also possible from corner to corner of a hypercube network that has three spins per edge (edge in the colloquial sense). The transfer time on such a network is $T = \frac{\pi}{\Omega_0\sqrt{2}}$.

Symmetric hypercube networks thus achieve perfect quantum state transfer in a time T *independent of the dimension* d, a result first reported by Christandl et. al. in [5], who also showed that perfect state transfer is achieved on hypercubes if each edge[7] of the cube has three vertices instead of two, as in Figure 1.4. The fidelity F as a function of time, though, is $F(t) = \sin^{2d}(\Omega_0 t)$, so the width of the peak in the fidelity gets narrower and as d increases.

Note that for intermediate times, the sender's excitation is delocalized over the entire hypercube: it traverses every path from sender to receiver. This fact makes hypercubes useful in other areas of quantum computation, such as quantum search algorithms [15]. Furthermore, while we will not explicitly consider the effects of network imperfections in this thesis, state transfer on hypercube networks has been shown to be unusually resistant to decoherence if each node's spin decoheres independently [16].

1.3 State Transfer via Quantum Teleportation

Another attractive alternative to photonic quantum communication uses entanglement to perform quantum teleportation. However, these schemes require that the sender and receiver already share maximally entangled pairs. This distribution of entangled pairs is nontrivial, but can be achieved using a well designed spin networks.

[7] "Edge" is used here in the colloquial sense.

1.3.1 Entanglement and Quantum Teleportation

Entanglement is a property of multi-particle quantum systems; if two qubits A and B are entangled, neither qubit has a full description (i.e. a state vector) of its own. The quintessential example of an entangled pair is the singlet spin state. Using the standard notation for spins, the singlet state is

$$|\Psi^-\rangle = \frac{1}{\sqrt{2}} \left(|\uparrow\rangle_A |\downarrow\rangle_B - |\downarrow\rangle_A |\uparrow\rangle_B \right). \tag{1.19}$$

If the spin of particle A is measured along an axis $\hat{\mathbf{n}}$ and the spin of particle B is subsequently measured along the same axis, the two measurement results will *always* be opposite, no matter what axis was chosen. This correlation in the results of any measurement of the entangled variables (spins, in this case) is the mark of entanglement. Because the measurement results are perfectly (anti-)correlated for the singlet state, it is maximally entangled. These maximally entangled states are also called Bell pairs, or Bell states, after John Bell who used them to demonstrate that quantum mechanic violates the principles of local realism [7].

Quantum entanglement is a physical resource. Entangled pairs are extremely useful, making possible superdense coding, quantum algorithms, and quantum teleportation [7]. Quantum teleportation, first reported in [17], is a process by which two parties, Alice and Bob, who share a maximally entangled pair can achieve perfect quantum communication. Suppose that Alice and Bob do share a Bell pair, and that Alice possess an arbitrary qubit state $|\psi\rangle$ that she wishes to transfer to Bob. By allowing her qubit to interact with her member of the entangled pair, performing measurements on her two qubits, and reporting the results to Bob, Bob can then perform local operations on his qubit to coerce it into the state $|\psi\rangle$ with perfect fidelity. This process does note violate the No-Cloning Theorem [9]: afterwards, Bob possesses a qubit in the state $|\psi\rangle$, but Alice no longer does (hence "teleportation").

1.3.2 Sharing Entangled Pairs

There is a cost to the teleportation process: it consumes the entangled pair originally shared by Alice and Bob. Teleportation does not remove the problem of quantum state transfer, but it does reduce it to one of distributing maximally entangled pairs.

Just as a spin network can be used to send states from one node to another (with some fidelity), it can be used to share entanglement. Suppose the sender is in possession of a maximally entangled pair of qubits A and A' in the state $|\Psi\rangle$. She can transfer one-half of this pair—say, qubit A'—to the receiver (with some fidelity) by keeping the first particle, A, decoupled from the spin network while placing the second particle, A', at her node at time $t = 0$. In other words, she keeps A separate from the network while arranging for particle A' to be her node qubit. State transfer then proceeds as before: sender and receiver allow the network to evolve for some time T, then the receiver decouples his qubit, which we will call B, from the network. Let $\rho_{AB}(T)$ be the density matrix for the (potentially mixed) state of the sender's qubit A and the receiver's qubit B. The sender can then perform a local unitary operation U_A

on her qubit A, and the receiver can perform a local unitary operation U_B on his qubit. The state of their shared pair after this procedure is $\widetilde{\rho}_{AB}(T) = U_A^\dagger \otimes U_B^\dagger \rho_{AB}(T) U_A \otimes U_B$. The fidelity of the entanglement transfer is just the fidelity of $\widetilde{\rho}_{AB}(T)$ with the Bell state $|\Psi\rangle$:

$$F_{s\to r}(T) = \langle \Psi | \widetilde{\rho}_{AB}(T) | \Psi \rangle, \tag{1.20}$$

Again, U_A, U_B and T are chosen to maximize the fidelity. If the fidelity is high, then the entanglement shared between the sender and receiver is also large. Any spin network that transfers entanglement with high fidelity can also be used to transfer single-qubit quantum states efficiently. Indeed, the fidelity for transferring entanglement is an upper bound for the average fidelity fidelity of single-qubit state transfer [18].

For example, entangled pairs can be perfectly transferred from corner to corner of the hypercube network discussed above in a time T. The time evolution operator $\mathcal{U}_t^{(tot)}$ for the entire system—sender's qubit A, and the spin network—is $\mathcal{U}_t^{tot} = I_A \otimes \mathcal{U}_t$, where $\mathcal{U}_t$ is the time evolution operator for the network. If the sender's initial pair is in the state $|\Phi^+\rangle = (|0\rangle_A |0\rangle_{A'} + |1\rangle_A |1\rangle_{A'})/\sqrt{2}$, then the system's state at time T is

$$|A, \text{network}(T)\rangle = (I_A \otimes \mathcal{U}_T) \left(\frac{|0\rangle_A |\text{vac}\rangle + |1\rangle_A |\mathbf{z}\rangle}{\sqrt{2}} \right) = \frac{|0\rangle_A |\text{vac}\rangle + (-i)^d |1\rangle_A |\overline{\mathbf{z}}\rangle}{\sqrt{2}}, \tag{1.21}$$

so the sender-receiver qubit pair AB is in the state $(|0\rangle_A |0\rangle_B + (-i)^d |1\rangle_A |1\rangle_B)/\sqrt{2}$. To recover the state $|\Phi^+\rangle$, each party would apply the operation $U = \left(\begin{smallmatrix} 1 & 0 \\ 0 & \sqrt{i^d} \end{smallmatrix}\right)$ to their qubit.

1.3.3 Entanglement Distillation

If sender s and receiver r are to achieve quantum communication by teleportation, then they need to share maximally entangled Bell states. After using the entanglement-sharing protocol described in the previous section, sender s and receiver r do not generally share a Bell state, but rather they share an approximate Bell state whose fidelity is given by (1.20).

If the sender and receiver first use the spin network to share n copies of the approximate Bell state $\widetilde{\rho}_{AB}$, they can then employ classical communication and local operations (including local measurements) to turn their collection of n approximate Bell pairs into a smaller collection of m perfect[8] Bell pairs. Such procedures, now known as *entanglement distillation*, were first proposed in [19]. The *yield* $Y(\widetilde{\rho}_{AB})$ of the distillation procedure is the ratio m/n as $n \to \infty$.

For example, in the original paper on entanglement distillation of mixed states, Bennett *et al.* [19] outline several (not necessarily optimal) protocols for distilling

[8]Really, if they are to achieve quantum communication with arbitrarily high fidelity, then they need to share states that are arbitrarily close to Bell states. Distillation processes turn non-maximally entangled states into states arbitrarily close to a Bell state.

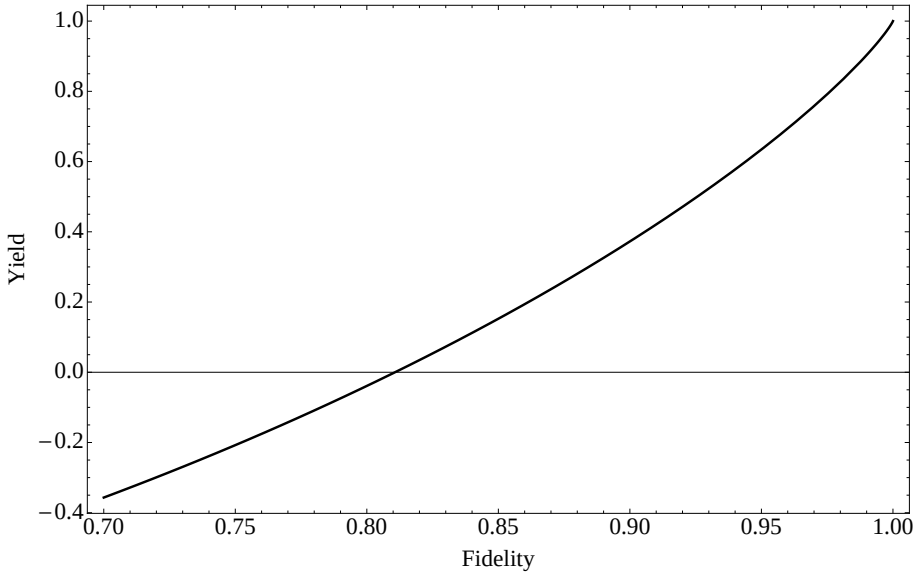

Figure 1.5: A plot of the yield $Y_0(F)$ of most efficient entanglement distillation procedure outlined in [19]; the procedure takes a large number of approximate Bell states and transforms them, via local operations and classical communication, into perfect Bell states.

mixed states ρ into perfect Bell states. The best of these has a yield Y_0 which can be written as a function of the Bell state fidelity F defined in (1.20) as

$$Y_0(F) = 1 + F \log_2 F + (1 - F) \log_2 \frac{1 - F}{3}, \tag{1.22}$$

The function $Y_0(F)$ is shown in Figure 1.5. It is nonnegative only for values of F greater than a critical value $F_{\text{crit}} \approx 0.81$; if the starting materials (approximate singlet states) have a singlet fidelity smaller than F_{crit}, distillation by this procedure cannot be performed.

The most meaningful characterization of the entanglement shared between sender S and receiver R in this situation is the *distillable entanglement*, $D(\widetilde{\rho}_{AB})$. The distillable entanglement is the maximum possible yield $Y(\widetilde{\rho}_{AB})$, i.e. it is the yield when an optimal distillation procedure is used. Roughly speaking, the distillable entanglement is the number of Bell pairs that the state $\widetilde{\rho}_{AB}$ can be turned into.

The distillable entanglement is the proper way to quantify the entanglement shared between the sender and receiver, however it is notoriously hard to calculate. In fact, the distillable entanglement $D(\rho)$ of an arbitrary two-qubit density matrix ρ is not known[9]. Because of this, we will use the fidelity (1.20) to quantify

[9]In the special case that the two-qubit density matrix is a pure state, $\rho = |\Psi\rangle\langle\Psi|$, the distillable entanglement is known to be equal to the entanglement of formation. The entanglement of formation of a state ρ is defined opposite the distillable entanglement: roughly, it's the number of Bell states needed to create the state ρ [7] . For more on measures of entanglement, see [20].

the entanglement transferred via the spin network. It is not quite as meaningful as the distillable entanglement shared between sender and receiver, but calculating the fidelity is tractable. Moreover, from the fidelity a lower bound on the distillable entanglement can be calculated by picking an entanglement distillation process and calculating the yield.

Chapter 2

Parallel State Transfer

2.1 Introduction

In the previous chapter quantum state transfer via spin networks was presented as a means for achieving quantum communication in a quantum computer. We considered how effectively a single quantum state could be transferred from one node of the network (the sender register) to another (the receiver register). That is, we focused on single quantum state transfer: transferring only a single qubit state along the quantum network. It would, of course, be much more efficient if many quantum states could be faithfully transmitted along the same network in parallel. In this chapter we ask: how effectively can multiple senders and receivers use the same quantum network at the same time? In other words, we consider the problem of parallel quantum state transfer.

As an example, consider a 3-dimensional cube network with equal couplings Ω_0. It was shown in Section 1.2.2 that if a d-cube is symmetric, that is, if all of the on-site energies Ω_{vv} are equal, then perfect state transfer is achievable from corner-to-corner in a time $T = \frac{\pi}{2\Omega_0}$ (Figure 2.1(a).). A 3-cube, though, is just two connected 2-cubes (squares). Can the 3-cube be broken up, split into two effectively decoupled 2-cube channels, so that faithful state transfer can be performed along each of these two channels at the same time? This situation is depicted in Figure 2.1(b). Alternatively, can the 3-cube be split into four effectively decoupled 1-cube channels (pairs), so that states can be transferred along each of these four channels at the same time, as in Figure 2.1(c)?

Unsurprisingly, the answer to both of these questions is an unequivocal "yes". The most important question, though, is this: for a given network, how do the errors scale as more and more users try to transfer states along the network in parallel?

In this chapter we address such questions, although we focus on the problem of parallel entanglement transfer instead of parallel state transfer. We first develop the language and tools necessary to study parallel entanglement transfer on *oscillator* networks. We then apply these methods to obtain analytical results for the fidelity of parallel entanglement transfer on hypercube networks of oscillators. In Section 2.4 we compare the analytical results for oscillator networks to numerical results for qubit

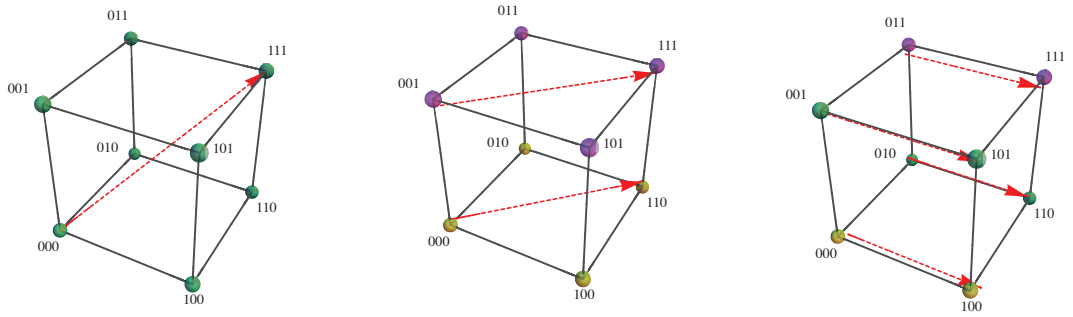

Figure 2.1: **(a):** Perfect state transfer is possible from corner to corner of a symmetric d-dimensional hypercube. **(b):** A 3-cube can be split up into two effectively decoupled 2-cube channels (opposing faces). **(c):** A 3-cube can also be split into four effectively decoupled 1-cube channels (pairs).

networks.

As in Chapter 1, we will restrict our attention to the case in which all of the network couplings are equal, but the on-site energies are programmable. We do not, therefore, allow that the couplings between the opposing faces of the cube in Figure 2.1(b) be literally turned off. If they could, the state transfer on each face would be perfect. The coupling can be made effectively weak, though, by detuning the on-site energies of the opposing faces: i.e., by making the energy difference between $|0\rangle$ and $|1\rangle$ on the left face much smaller than the energy difference between $|0\rangle$ and $|1\rangle$ on the right face.

2.2 Oscillator Networks

2.2.1 Motivation

In studying parallel quantum state transfer we shift our attention from spin networks, which have a qubit at each node, to oscillator networks with an harmonic oscillator at each node. The dynamics of oscillators networks are vastly simpler than the dynamics of spin networks. While it is natural to study single state transfer entirely in the network's single excitation subpsace, parallel state transfer is necessarily studied in this and higher excitation subspaces. As we shall see, the dynamics of the single-excitation subspace directly control the dynamics of every other state for oscillator networks. Spin networks, however, are still of great interest, and in Section 2.4 we present numerical evidence that the fidelity of parallel entanglement transfer on oscillator networks is, under some circumstances, qualitatively similar to parallel entanglement transfer on spin networks. To some extent, then, this shift of focus is

for computational convenience, partially justified by the numerical evidence presented in Section 2.4.

Still, if realized, oscillator networks would have some distinct theoretical advantages over spin networks. In particular, we will show that truly perfect parallel entanglement transfer is possible on oscillator networks, while we believe that it is not on spin networks. Furthermore, as will be discussed in Section 2.4.2, entanglement can be distributed on hypercube oscillator networks in a *massively* parallel sense not achievable on the corresponding spin networks.

On the other hand, there are challenges to physically realizing oscillator networks. A main motivation for studying spin networks was to find a non-photonic means of achieving quantum state transfer in a quantum computer. By using networks of qubits, the connections between registers could be built from the same components as the registers themselves, eliminating the need for an interface between the network and the registers. Oscillators networks abandon this principal, so implementation is more difficult, and does require an interface between the oscillators that make up the network and the qubits within the register. Recently, such an interface between superconducting Josephson junction qubits and a microwave resonator was demonstrated by the Martinis group to prepare the resonator in arbitrary superpositions of Fock states [6]. A protocol based on this work has also been designed for synthesizing arbitrary entangled states of two oscillators [21].

2.2.2 The Parallel State Transfer Protocol

Suppose that the registers of a quantum computer are connected by an oscillator network with network graph $\mathcal{G} = (V, E)$ that is to be used for quantum state transfer. Consider first the situation in which, during a given "use" of the network, there is only a single pair of users, sender and receiver. Just as in Section 1.3, the sender wishes to use the network to transfer half of a Bell state to the receiver (with some fidelity), repeat the process many times, distill the shared approximate Bell pairs into perfect Bell pairs, and then communicate via teleportation. For simplicity, we will assume that the entangled pair that the sender starts with is a qubit, A, entangled with her oscillator, s. The joint state of the qubit-oscillator pair is some Bell state $|\Psi\rangle$. The sender and receiver could use the following protocol in order to (attempt to) achieve entanglement transfer.

Single User Entanglement Transfer on an Oscillator Network

Step 1: The sender is in possession of a qubit-oscillator pair in a Bell state $|\Psi\rangle$. The rest of the network is in some initial state $|\text{not } s\rangle$.

Step 2: The oscillator network is allowed to evolve according to the natural time evolution of its Hamiltonian for some time T (the transfer time). The sender's qubit A is kept isolated, so that it does not evolve in time.

Step 3: The receiver transfers the state of his oscillator to a qubit B in his possession.

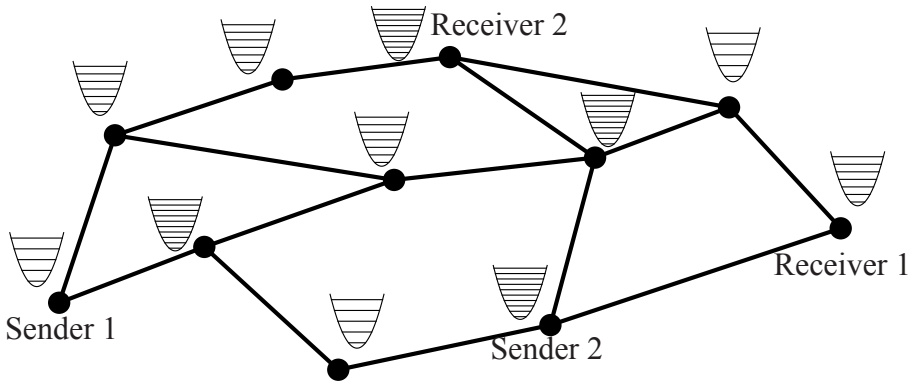

Figure 2.2: An oscillator network being used by two senders and two receivers.

Step 4: The sender and receiver each perform local operations U_A and U_B on their qubits A and B. The state of the qubit pair AB is now denoted by $\widetilde{\rho}_{AB}(T)$.

The fidelity of the entanglement transfer is, as before, given by $\langle\Psi|\widetilde{\rho}_{AB}(T)|\Psi\rangle$. An obvious choice for the initial state of the non-sender oscillators is to have them all in the ground state: $|\text{not } s\rangle = |00\ldots00\rangle$. However, we stress that this is not necessary—the state $|\text{not } s\rangle$ could be anything.

Now consider the same network being used for parallel entanglement transfer. In a given use of the network, some vertices act as senders and some as receivers, as in Figure 2.2. Let $S = \{s_1, \ldots, s_M\}$ be the set of vertices with senders, and $R = \{r_1, \ldots, r_M\}$ be the set of vertices with corresponding receivers[1]. The protocol that we will study for parallel entanglement transfer is as follows.

Parallel Entanglement Transfer on an Oscillator Network

Step 1: Each sender s_j is in possession of a qubit-oscillator pair in a Bell state $|\psi\rangle$. Every oscillator not associated with a sender is in the state $|0\rangle$.

Step 2: The oscillator network is allowed to evolve according the the natural time evolution of its Hamiltonian for some time T (the transfer time). Each sender's qubit A_j is kept isolated, so that it does not evolve in time.

Step 3: Each receiver r_j transfers the state of his oscillator to a qubit B_j in his possession.

Step 4: The sender s_j and receiver r_j each perform local operations U_{A_j} and U_{B_j} on their qubits A_j and B_j. The state of the qubit pair A_jB_j after these unitary operations have been performed is denoted by $\widetilde{\rho}_{A_jB_j}(T)$.

[1]There is, in general, no reason why there must be the same number of senders as receivers. However, we will only consider casesin which there are.

As perceived by a single pair of users (sender s_j and receiver r_j), the parallel state transfer protocol is exactly the same as the single state transfer protocol, but with the quantum state of the rest of the network, $|\text{not } s_j\rangle$, determined by the states that the other senders are trying to transfer. In this sense there is not much of a conceptual difference between single state transfer and parallel state transfer. Thus we can quantify the faithfulness of the transfer, as far as a particular pair sender s_j and receiver r_j is concerned, in exactly the same way as for the spin networks discussed in Section 1.2: by the fidelity $F_{s_j \to r_j}(T)$ of $\widetilde{\rho}_{A_j B_j}(T)$ with $|\Psi\rangle$,

$$F_{s_j \to r_j}(T) = \langle \Psi | \widetilde{\rho}_{A_j B_j}(T) | \Psi \rangle. \tag{2.1}$$

Step 4 of our state transfer protocols for oscillator networks involve the receiver(s) "unloading" an oscillator state from the network to a qubit. To achieve this, the receiver can use the unitary operation U_{SWAP},

$$U_{\text{SWAP}} = \sum_{n=0}^{\infty} |1, n\rangle\langle 0, n+1| + \sum_{n=0}^{\infty} |0, n+1\rangle\langle 1, n| + |0, 0\rangle\langle 0, 0|, \tag{2.2}$$

on his qubit-oscillator pair. Here $|q, n\rangle = |q\rangle_{\text{qubit}} \otimes |n\rangle_{\text{oscillator}}$. The operation U_{SWAP} is indeed unitary since

$$U_{\text{SWAP}}^{\dagger} U_{\text{SWAP}} = |0, 0\rangle\langle 0, 0| + \sum_{n=0}^{\infty} |0, n+1\rangle\langle 0, n+1| + \sum_{n=0}^{\infty} |1, n\rangle\langle 1, n| = \mathcal{I}, \tag{2.3}$$

and is thus an allowed quantum mechanical transformation. In fact, as mentioned above, similar transformations have been realized experimentally using superconducting qubits and microwave resonators [6].

2.2.3 The Hamiltonian and Time Evolution

Just as we consider only spin networks with equal couplings and programmable on-site energies, we only consider oscillator networks with equal couplings and programmable energy level spacings. The Hamiltonian for such an equal coupling oscillator network with network graph $\mathcal{G} = (V, E)$ can be written terms of the creation and annihilation operators $a_v^{\dagger}$ and a_v for the oscillator at node v as

$$\mathcal{H} = \hbar \sum_{v \in V} \Omega_{vv} a_v^{\dagger} a_v + \hbar \Omega_0 \sum_{\{u,v\} \in E} \left(a_u^{\dagger} a_v + a_v^{\dagger} a_u \right). \tag{2.4}$$

Again, Ω_0 is the constant coupling strength and the Ω_{vv}'s are the energy level spacings, which we consider programmable: the senders and receivers using the oscillator network can control them, and can change them from one use of the network to another. The Hamiltonian, then, is completely specified by the Ω matrix. The term $a_u^{\dagger} a_v + a_v^{\dagger} a_u$ in the Hamiltonian couples the oscillators at nodes u and v together, and is the natural analog of the XY coupling for spin networks that was considered in Chapter 1. Indeed, the XY coupling for spins can, equivalently, be written as

$$\frac{1}{2} \left(\sigma_x^{(u)} \sigma_x^{(v)} + \sigma_y^{(u)} \sigma_y^{(v)} \right) = \sigma_+^{(u)} \sigma_-^{(v)} + \sigma_-^{(u)} \sigma_+^{(v)}, \tag{2.5}$$

where $\sigma_{\pm}^{(v)}$ is the usual ladder operator $\sigma_{\pm}^{(v)} = \frac{1}{2}(\sigma_x^{(v)} \mp i\sigma_y^{(v)})$ for the qubit at site v in the corresponding spin network.

Matrix Elements of the Time Evolution Operator $\mathcal{U}_t$

The Hamiltonian (2.4) is again time independent so the time evolution operator $\mathcal{U}_t$ is given by

$$\mathcal{U}_t = e^{-i\mathcal{H}t/\hbar}. \tag{2.6}$$

Calculating the time evolution operator might seem hopelessly difficult. However, by examining things in the Heisenberg picture, we can reduce the task of exponentiating the full Hamiltonian $\mathcal{H}$ (an infinite dimensional operator on the network space) to exponentiating only the matrix Ω (a finite dimensional operator on graph space).

The Heisenberg equation of motion for the annihilation operator a_v is:

$$\begin{aligned}\frac{d}{dt}a_v(t) &= \frac{i}{\hbar}\left[\mathcal{H}, a_v(t)\right] \\ &= i\Omega_{vv}[a_v^\dagger a_v, a_v(t)] + i\sum_{v'\neq v}\Omega_{vv'}[a_v^\dagger a_{v'} + a_{v'}^\dagger a_v, a_v(t)] \\ &= -i\sum_{v'}\Omega_{vv'}a_{v'}.\end{aligned} \tag{2.7}$$

This is a set of N coupled differential equations, one for each oscillator, which can be written in matrix form as:

$$\frac{d}{dt}\begin{pmatrix} a_{v_1} \\ a_{v_2} \\ \vdots \\ a_{v_N}\end{pmatrix}(t) = -i\underbrace{\begin{pmatrix} \Omega_{v_1v_1} & \Omega_{v_1v_2} & \cdots & \Omega_{v_1v_N} \\ \Omega_{v_2v_1} & \Omega_{v_2v_2} & \cdots & \Omega_{v_2v_N} \\ \vdots & \vdots & \ddots & \vdots \\ \Omega_{v_Nv_1} & \Omega_{v_Nv_2} & \cdots & \Omega_{v_Nv_N}\end{pmatrix}}_{\text{The } \Omega \text{ matrix!}}\begin{pmatrix} a_{v_1} \\ a_{v_2} \\ \vdots \\ a_{v_N}\end{pmatrix}(t). \tag{2.8}$$

These have the formal solution

$$\begin{pmatrix} a_{v_1} \\ a_{v_2} \\ \vdots \\ a_{v_N}\end{pmatrix}(t) = \begin{pmatrix} \mathbb{K}_{v_1v_1} & \mathbb{K}_{v_1v_2} & \cdots & \mathbb{K}_{v_1v_N} \\ \mathbb{K}_{v_2v_1} & \mathbb{K}_{v_2v_2} & \cdots & \mathbb{K}_{v_2v_N} \\ \vdots & \vdots & \ddots & \vdots \\ \mathbb{K}_{v_Nv_1} & \mathbb{K}_{v_Mv_2} & \cdots & \mathbb{K}_{v_Nv_N}\end{pmatrix}\begin{pmatrix} a_{v_1} \\ a_{v_2} \\ \vdots \\ a_{v_N}\end{pmatrix}(t=0), \tag{2.9}$$

where $\mathbb{K} = e^{-i\Omega t}$ is the mode evolution operator, an operator on graph-space. Since any state in the network space can be written in terms of creation operators, we can use (2.9) to write matrix elements of $\mathcal{U}_t$ in terms of matrix elements of $\mathbb{K}$. We will denote the ℓ-excitation subspace state $\chi a_{v_1}^\dagger a_{v_2}^\dagger \ldots a_{v_\ell}^\dagger|\text{vac}\rangle$ by $|v_1v_2\ldots v_\ell\rangle$ (here χ is a normalization constant, necessary if any of the v_j's are repeated). In particular, if all of the v_j's and v_j''s are distinct, then

$$\begin{aligned}\langle v_1' \cdots + v_\ell'|\mathcal{U}_t|v_1 \cdots + v_\ell\rangle =& \langle\text{vac}|a_{v_1'}\ldots a_{v_\ell'}\mathcal{U}_t a_{v_1}\ldots a_{v_\ell}|\text{vac}\rangle \\ =& \langle\text{vac}|a_{v_1'}\ldots a_{v_\ell'}(\mathcal{U}_t a_{v_1}\mathcal{U}_t^\dagger)\ldots(\mathcal{U}_t a_{v_\ell}\mathcal{U}_t^\dagger)\mathcal{U}_t|\text{vac}\rangle \\ =& \langle\text{vac}|a_{v_1'}a_{v_2'}\ldots a_{v_\ell'}a_{v_1}(t)^\dagger\ldots a_{v_\ell}(t)^\dagger|\text{vac}\rangle\end{aligned} \tag{2.10}$$

Since $a_v(t)^\dagger = \sum_w \langle w|\mathbb{K}^\dagger|v\rangle_{\mathcal{G}} a_w^\dagger$ there are *many* nonzero terms hiding in the right-hand-side of (2.10). The most obvious term occurs when $a_{v_1}^\dagger$ "turns into" $a_{v_1'}^\dagger$, and $a_{v_2}^\dagger$ "turns into" $a_{v_2'}^\dagger$, etc. However, every permutation of the operators $a_{v_1}^\dagger \dots a_{v_\ell}^\dagger$ turning into the operators $a_{v_1'}^\dagger \dots a_{v_\ell'}^\dagger$ contributes; for example, if $a_{v_1}^\dagger$ turns into $a_{v_2'}^\dagger$, $a_{v_2}^\dagger$ turns into $a_{v_1'}^\dagger$, and $a_{v_j}^\dagger$ turns into $a_{v_j'}^\dagger$ for all other j. Thus, we can write the matrix element of $\mathcal{U}_t$ from (2.10) as

$$\langle v_1' + v_2' \dots v_\ell'|\mathcal{U}_t|v_1 + v_2 \dots v_\ell\rangle = \sum_{\substack{\text{permutations} \\ \pi}} \prod_{i=1}^{\ell} \langle v_i'|\mathbb{K}^\dagger|v_{\pi(i)}\rangle_{\mathcal{G}}. \tag{2.11}$$

We mention that the right-hand-side (2.11) is the definition of the *permanent* of the $\ell \times \ell$ matrix whose elements are $\langle v_j'|\mathbb{K}^\dagger|v_j\rangle$. If all the v_j's are distinct, and all of the v_j''s are distinct *except* for p of them, then the matrix element is

$$\langle v_1' + v_2' \dots v_\ell'|\mathcal{U}_t|v_1 + v_2 \dots v_\ell\rangle = \sqrt{p!} \sum_{\substack{\text{permutations} \\ \pi}} \prod_{i=1}^{\ell} \langle v_i'|\mathbb{K}^\dagger|v_{\pi(i)}\rangle_{\mathcal{G}}. \tag{2.12}$$

This is the beauty of oscillator networks: a matrix element of $\mathcal{U}_t$ in the ℓ-excitation subspace can be expanded as a sum of products of matrix elements of $\mathbb{K}$, with $\ell!$ terms in the sum. The dynamics of an arbitrary state in the infinite dimensional network space are governed by a finite dimensional operator on graph-space. If all the diagonal entries of the Ω matrix are zero, then the dynamics of the oscillator network are controlled by the adjacency matrix of the network graph $\mathcal{G}$.

In contrast, the situation for spin networks is much more complicated. If the diagonal entries of the Ω matrix are zero, then, as shown in Section 1.2.1, the adjacency matrix of $\mathcal{G}$ directly controls the single-excitation subspace. This adjacency matrix, however, does not directly control the dynamics of higher excitation subspaces. It turns out that the ℓ-excitation dynamics are governed by the adjacency matrix of $\wedge^\ell\mathcal{G}$, the ℓ^{th} wedge product of $\mathcal{G}$ with itself. The spectral properties of $\wedge^\ell\mathcal{G}$, however, are not generally known to be related to those of $\mathcal{G}$ in any simple manner [22].

2.3 Parallel Entanglement Transfer on Hypercubes Networks

2.3.1 Channels, Senders, and Receivers

We now analyze the hypercube network's capacity for parallel entanglement transfer. The d-dimensional hypercube graph has as its vertex set the set of bitstrings of length d, and two vertices are connected if their bitstrings differ in exactly on place (see Section 1.2.2).

As depicted in Figure 2.1 for the 3-cube, a d-dimensional hypercube can be naturally broken apart into subcube channels: the d-cube can be divided into two $(d-1)$-cubes; each $(d-1)$-cube can be divided into two $(d-2)$-cubes; each of these can be

divided into two $(d-3)$-cubes, and so on. We are thus led to consider the question of dividing the d-dimensional hypercube into $M = 2^m$ channels, with each channel a $(d-m)$-dimensional subcube.

Given a bitstring[2] $\mathbf{x}$ of length m, we define the channel $C_{\mathbf{x}}$ to be the set of vertices on the d-cube that end in $\mathbf{x}$:

$$C_{\mathbf{x}} = \{\mathbf{yx} | \mathbf{y} = y_d \dots y_{m+1} \in \mathbb{Z}_2^{(d-m)}\}. \tag{2.13}$$

(Remember: our convention is to label the bits of a bitstring *from right to left.*) Channels, as defined in this way, really are subcubes of dimension $(d-m)$. For any vertex $\mathbf{z}$ of the d-cube, the right-most m bits label which channel the vertex is on and the left-most $(d-m)$ bits of $\mathbf{z}$ label position on the channel:

$$\mathbf{z} = \underbrace{z_d \dots z_{m+1}}_{\substack{\text{position on} \\ \text{channel}}} \underbrace{z_m \dots z_1}_{\text{channel}}. \tag{2.14}$$

Finally, note that the channels themselves have the structure of an m-cube. Defining two channels $C_{\mathbf{x}}$ and $C_{\mathbf{x}'}$ to be adjacent if they are distinct and if $C_{\mathbf{x}}$ contains a vertex adjacent to some vertex of $C_{\mathbf{x}'}$, we see that the two channels are adjacent if and only if $\mathbf{x}$ and $\mathbf{x}'$ differ, as bitstrings, in exactly one place. In other words, the two channels are adjacent if and only if $\mathbf{x}$ and $\mathbf{x}'$ are adjacent vertices on an m-cube. Thus, the channels are subcubes of the d-dimensional network cube, and the channels are also connected in a cubelike manner.

Can one sender per channel—$M = 2^m$ senders in total—use the oscillator network to transfer entanglement with a receiver at the opposite end of that channel via the parallel transfer protocol discussed in Section 2.2.2? In particular, let $\mathbf{s} = 00\dots00$ be a bitstring of $(d-m)$ 0's and $\mathbf{r} = 11\dots11$ be a bitstring of $(d-m)$ 1's. Define the sender set S as

$$S = \{\mathbf{sx} | \mathbf{x} \in \mathbb{Z}_2^m\} \tag{2.15}$$

and the receiver set R as

$$R = \{\mathbf{rx} | \mathbf{x} \in \mathbb{Z}_2^m\}. \tag{2.16}$$

Then our question becomes: can entanglement be transferred with a high fidelity $F_{\mathbf{sx}\to\mathbf{rx}}$ for each $\mathbf{x}$? Note, by the way, that the senders and receivers defined here are all transferring entanglement in the same direction along their channels, as in Figure 2.1. This means that the sets S and R are also subcubes of dimension m. We will sometimes refer to these as the Senders' Cube and the Receivers' Cube. The channel C_{000}, the Senders' Cube S and the Receivers' Cube R are shown in Figure 2.3 for a $d = 5$ network intended for $M = 2^3$ senders and $M = 2^3$ receivers.

[2]Bitstrings abound. Generally, we use $\mathbf{z}$ as a bitstring of length d, $\mathbf{y}$ as a bistring of length $(d-m)$, and $\mathbf{x}$ as the (soon to be ubiquitous) bitstring of length m.

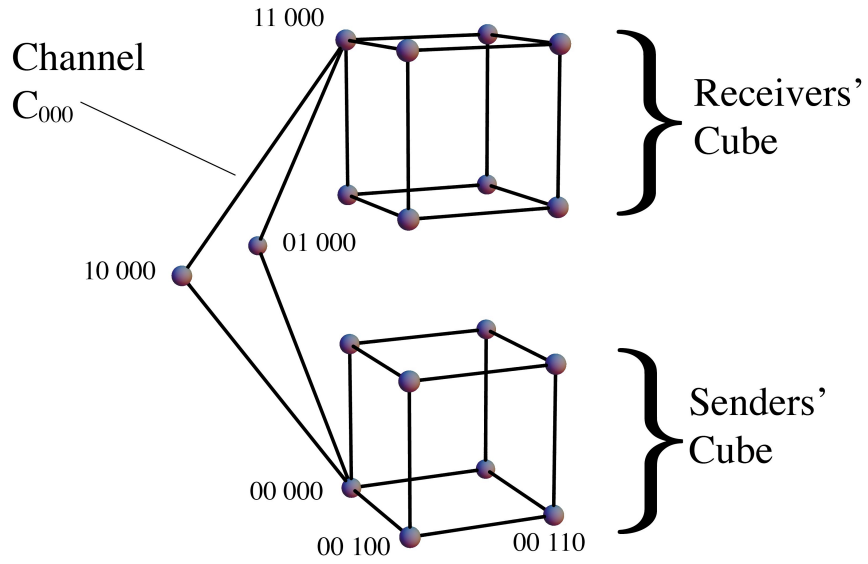

Figure 2.3: A hypercube oscillator network with $d = 5$ and $m = 3$ ($N = 2^3$). Only the Senders' Cube, Receivers' Cube, and channel C_{000} are shown. Seven channels are missing, as are links between channels.

2.3.2 Decoupling Adjacent Channels

In order for sender **sx** to faithfully transfer entanglement with the corresponding receiver **rx**, we expect that channel $C_{\mathbf{x}}$ must be effectively decoupled from adjacent channels. This effective decoupling can be achieved by detuning the oscillator energies for channel $C_{\mathbf{x}}$ far from the energies for adjacent channels. There are many ways to achieve this. One particularly simple method is to pick the diagonal portion of the Ω matrix in (2.4) to be

$$\Omega^{(\mathrm{diag})} = \omega_0 I + \frac{1}{2}\Delta\omega \sum_{j=1}^{m} Z^{(j)}. \tag{2.17}$$

Here $Z^{(j)}$ denote the Pauli z-spin matrix on bit j— it's action on a vector in graph-space is:

$$Z^{(j)}|z_d z_{d-1} \ldots z_j \ldots z_2 z_1\rangle_{\mathcal{G}} = \begin{cases} +|z_d z_{d-1} \ldots z_j \ldots z_2 z_1\rangle_{\mathcal{G}} & \text{if } z_j = 0 \\ -|z_d z_{d-1} \ldots z_j \ldots z_2 z_1\rangle_{\mathcal{G}} & \text{if } z_j = 1 \end{cases}. \tag{2.18}$$

Again, the off-diagonal portion of the Ω-matrix is just a multiple of the adjacency matrix for the network graph, so we have

$$\Omega = \omega_0 I + \frac{1}{2}\Delta\omega \sum_{j=1}^{m} Z^{(j)} + \Omega_0 \sum_{j=1}^{d} X^{(j)}. \tag{2.19}$$

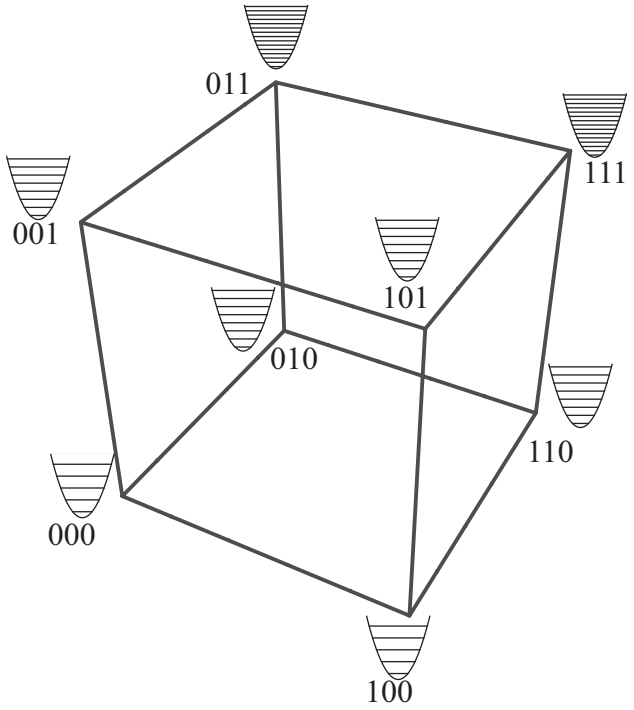

Figure 2.4: The splitting scheme of (2.17) depicted for $m = 2$ ($M = 2^2$ senders) on a $d = 3$ cube.

The splitting scheme of (2.17) is the scheme we will study. Using this scheme, the spacing $\Omega_{\mathbf{xx}}$ for channel $C_{\mathbf{x}}$ differs by an amount $\pm\Delta\omega$ from adjacent channels, and a channel's energy spacing depends only on the Hamming weight of the bitstring labelling the channel (the Hamming weight $w_H(\mathbf{x})$ of a bitstring $\mathbf{x}$ is its distance from the zero bitstring: $w_H(\mathbf{x}) = d_H(\mathbf{x}, 0\ldots0)$). Note that under this splitting, *not all channels are equivalent*. In particular, there is only one channel that has energy level spacings $\omega_0 + \frac{1}{2}m\Delta\omega$ (the channel $C_{0\ldots0}$), and each of the m channels adjacent to it has smaller energy level spacings. This decoupling scheme is depicted for $m = 2$ and $d = 3$ in Figure 2.4.

2.3.3 Calculating the Mode Evolution Operator $\mathbb{K}$

Since the Ω matrix in (2.19) for the hypercube network is a sum of commuting matrices, the exponential of this sum is just the product of the exponentials of each

term:

$$\begin{aligned}\mathbb{K} =& \exp\left[-i(\omega_0 I + \sum_{j=1}^{m}\left(\Omega_0 X^{(j)} + \frac{1}{2}\Delta\omega Z^{(j)}\right) + \Omega_0 \sum_{j=m+1}^{d} X^{(j)})t\right] \\ =& e^{-i\omega_0 t}\prod_{j=1}^{m}\exp\left[-i(\Omega_0 X^{(j)} + \frac{1}{2}\Delta\omega Z^{(j)})t\right]\prod_{j=m+1}^{d}\exp\left[-i\Omega_0 X^{(j)}t\right]. \end{aligned} \tag{2.20}$$

Using the identity $e^{-i\hat{\boldsymbol{n}}\cdot\vec{\boldsymbol{\sigma}}\theta} = I\cos\theta - (\hat{\boldsymbol{n}}\cdot\vec{\boldsymbol{\sigma}})\sin\theta$, one can show that:

$$\exp\left[-i\Omega_0 X^{(j)}t\right] = \cos(\Omega_0 t)I - i\sin(\Omega_0 t)X^{(j)} \tag{2.21}$$

$$\exp\left[-i\Omega_0 X^{(j)}t - i\frac{1}{2}\Delta\omega Z^{(j)}t\right] = \cos(\xi_t)I - i\sin(\xi_t)\left(n_x X^{(j)} + n_z Z^{(j)}\right), \tag{2.22}$$

where $n_x = \frac{\eta}{\sqrt{1+\eta^2}}$, $n_z = \frac{1}{\sqrt{1+\eta^2}}$, $\xi_t = \frac{1}{2}\Delta\omega t\sqrt{1+\eta^2}$, and $\eta = \frac{2\Omega_0}{\Delta\omega}$ is a parameter that controls the strength of the effective coupling between channels: small η corresponds to weak channel coupling. The mode evolution operator $\mathbb{K}$ can then be written as:

$$\begin{aligned}\mathbb{K} =& e^{-i\omega_0 t}\prod_{j=1}^{m}\left(\cos(\xi_t)I - i\sin(\xi_t)\left(n_x X^{(j)} + n_z Z^{(j)}\right)\right) \\ &\times \prod_{j=m+1}^{d}\left(\cos(\Omega_0 t)I - i\sin(\Omega_0 t)X^{(j)}\right)\end{aligned} \tag{2.23}$$

Together with (2.12), the expression for matrix elements of $\mathcal{U}_t$ in terms of elements of $\mathbb{K}$, we now know how to determine the dynamics of any state. Observe the time evolution of $|\mathbf{sx}\rangle$, a state in the single excitation subspace of the network space:

$$\mathcal{U}_t|\mathbf{sx}\rangle = \sum_{\mathbf{y}\in\mathbb{Z}_2^d}\langle\mathbf{y}|\mathbb{K}^\dagger|\mathbf{sx}\rangle_{\mathcal{G}}|\mathbf{y}\rangle. \tag{2.24}$$

An excitation that starts at sender $\mathbf{sx}$ will travel towards receiver $\mathbf{rx}$, as the $\sin\Omega_0 t$ grows in $\mathbb{K}$. If η, and hence n_x, is nonzero, some of the excitation leaks from sender $\mathbf{sx}$'s channel over to other channels. Each time the excitation "hops" from one channel to another, it picks up an extra factor of $n_x \approx \eta$. As long as the coupling parameter η is small, excitations more or less stay confined to channel on which they started[3]. The probability that receiver $\mathbf{rx}$'s oscillator is in the state $|1\rangle$ is, as a function of time is and to second order in η,

$$|\langle\mathbf{rx}|\mathcal{U}_t|\mathbf{sx}\rangle|^2 = |\langle\mathbf{rx}|\mathbb{K}^\dagger|\mathbf{sx}\rangle_{\mathcal{G}}|^2 = (1 - m\eta^2\sin^2\xi_t)\sin^{2(d-m)}\Omega_0 t \tag{2.25}$$

This probability is maximized at $t = \frac{\pi}{2\Omega_0}$, so we pick this as the transfer time T. In fact, the excitation is entirely localized on the Receivers' Cube at the transfer time T, as the $\cos\Omega_0 t$ in $\mathbb{K}$ has vanished.

[3]This is why we call the subcube $C_{\mathbf{x}}$ the channel between sender $\mathbf{sx}$ and receiver $\mathbf{rx}$. However, "channel" also has a much more technical meaning in quantum communications as any completely positive map between density matrices. We stress that we are *not* using channel in that sense.

Moreover, because every ℓ-excitation subspace matrix element is a product of single excitation subspace elements, if an ℓ-excitation subspace starts out localized on the Senders' Cube at time $t = 0$, it will be localized at the Receivers' Cube at $t = T$, for all ℓ. In this sense, the oscillator network can be thought of as a non-dispersive medium, and this fact allows for *perfect parallel state transfer* on the cube. The undesirable hopping terms can be eliminated if $\sin^2 \xi_T = 0$, which amounts to picking

$$\eta = \frac{1}{\sqrt{(2n)^2 - 1}} \qquad n = 1, 2, 3, \ldots \qquad \text{(perfect parallel transfer condition)} \tag{2.26}$$

If this condition is met, then the creation operator $a^\dagger_{\mathbf{sx}}$ evolves into *only* the creation operator $a^\dagger_{\mathbf{rx}}$ at time T, and excitations do not hop at all from one cube to the other.

While perfect parallel state transfer (and entanglement transfer) is achievable if the network builders have perfect control over the effective coupling parameter η, we would like to know how much error there is if η is off by just a bit, and in particular, how the error scales as a function of the number of users.

2.3.4 Fidelity: A Lower Bound

We now turn to calculating a lower bound on the fidelities of the parallel entanglement transfer for $M = 2^m$ senders using the protocol of Section 2.2.2 on the d-dimensional hypercube network with Hamiltonian specified by (2.19). We will focus on the weak coupling ($\eta \ll 1$) regime, and derive results correct to second order in η. For simplicity, we will assume that all the senders are attempting to transfer the triplet state $|\Phi^+\rangle = \frac{1}{\sqrt{2}}(|00\rangle + |11\rangle)$.

Still, the notation is about to get rather unwieldy—but bear with us, it's worth the effort! To calculate the fidelity for the pair sender **sx** and receiver **rx**, we need to keep track of the states of the 2^m sender qubits, the entire oscillator network, and receiver **rx**'s qubit, too. We don't need to worry about the other receivers' qubits—each receiver unloads his oscillator onto a qubit (with U_{SWAP}—(2.2)), but we can imagine that receiver **rx** unloads his oscillator first and calculate the fidelity $F_{\mathbf{sx}\to\mathbf{rx}}$ at that instant. This fidelity won't change when the other receivers perform local operations on their qubit-oscillator pairs.

We will call the collection of sender qubits, the oscillator network, and receiver **rx**'s qubit "the system", and we will denote the quantum state of the system at time t as $|\text{system}(t)\rangle$. We will write states in the system's state-space as the tensor product of three kets. The first ket refers to the spin state of the qubit pair $A_{\mathbf{x}}B_{\mathbf{x}}$ shared between sender **sx** and receiver **rx**. The second ket refers to the state of the other sender qubits, and the third ket refers to oscillator network. For example:

$$\underbrace{|01\rangle}_{A_{\mathbf{x}}B_{\mathbf{x}}} \underbrace{|\mathbf{sx}_1 + \mathbf{sx}_2 + \mathbf{sx}_3\rangle}_{\substack{\text{other}\\ \text{sender qubits}}} \underbrace{|\mathbf{rx}_1 + \mathbf{rx}_2 + \mathbf{rx}_4\rangle}_{\substack{\text{oscillator}\\ \text{network}}}. \tag{2.27}$$

But remember: **sx** and **rx** are the special pair, the sender and receiver whose entanglement transfer fidelity we are calculating.

The Vectors $|\psi_{jk}\rangle$

We can write the initial state of the system in terms of creation operators (for oscillators) and ladder operators (for spins) as

$$|\text{system}(0)\rangle = \left(\frac{1}{\sqrt{2}}\right)^M \prod_{\mathbf{x}} \left(1 + a^\dagger_{\mathbf{sx}}\, \sigma^{\mathbf{sx}}_+\right) |\text{vac}\rangle, \tag{2.28}$$

where the product is over all bitstrings $\mathbf{x}$ of length m; i.e. over all the sender vertices. At the transfer time T, all excitations on oscillator network have travelled over to the Receivers' Cube. After receiver $\mathbf{rx}$ has unloaded his oscillator (but before the sender and receiver have applied any other local unitaries), we can write the state of the system as

$$|\text{system}(T)\rangle = \frac{1}{\sqrt{2}}\Big(|00\rangle|\psi_{00}\rangle + |11\rangle|\psi_{11}\rangle\Big) + |01\rangle|\psi_{01}\rangle + |10\rangle|\psi_{10}\rangle, \tag{2.29}$$

where the $|\psi\rangle$'s are non-normalized states of the collection of senders' qubits and the oscillator network. The vector $|\psi_{jk}\rangle$ corresponds to all the ways that $|\text{system}(0)\rangle$ could evolve into into a state that leaves the qubit pair shared by sender $\mathbf{sx}$ and receiver $\mathbf{rx}$ in the state $|jk\rangle$ as Figure 2.5 illustrates.

For example, half of the terms in $|\text{system}(0)\rangle$ represent system configurations in which sender $\mathbf{sx}$'s qubit is in the $|0\rangle$ state. The non-normalized vector $|\psi_{00}\rangle$ includes terms for all possible ways that these configurations can evolve into configurations which leave receiver $\mathbf{rx}$'s oscillator, and hence his qubit after application of U_{SWAP}, in the state $|0\rangle$. Because at time T all excitations are localized on the Receivers' Cube, we can write $|\psi_{00}\rangle$ as

$$|\psi_{00}\rangle = \frac{1}{\sqrt{2^{M-1}}} \sum_{\ell=0}^{M-1} \sum_{\{\mathbf{x}_1 \ldots \mathbf{x}_\ell\}}{}' \overline{\sum_{\{\mathbf{x}'_1 \ldots \mathbf{x}'_\ell\}}{}'} \langle \mathbf{rx}'_1 \ldots \mathbf{rx}'_\ell | \mathcal{U}_T | \mathbf{sx}_1 \ldots \mathbf{sx}_\ell \rangle |\mathbf{sx}_1 \ldots \mathbf{sx}_\ell\rangle |\mathbf{rx}'_1 \ldots \mathbf{rx}'_\ell\rangle. \tag{2.30}$$

The first sum is over excitation number. The second sum is over senders, ℓ-element sets of bitstrings, and the prime denotes that the bitstring $\mathbf{x}$, corresponding to sender $\mathbf{sx}$, is to be left out. The third sum is over receivers, ℓ-element *multisets* of bitstrings. A multiset is a set in which elements can be repeated. That the third sum is over multisets merely reflects that a single oscillator can hold multiple excitations. The overbar denotes that the sum is over multisets instead of sets, and the prime again denotes that the bitstring $\mathbf{x}$ is to be left out.

The vector $|\psi_{11}\rangle$ can be written very similarly:

$$|\psi_{11}\rangle = \frac{1}{\sqrt{2^{M-1}}} \sum_{\ell=0}^{M-1} \sum_{\{\mathbf{x}_1 \ldots \mathbf{x}_\ell\}}{}' \overline{\sum_{\{\mathbf{x}'_1 \ldots \mathbf{x}'_\ell\}}} \langle \mathbf{rx} + \mathbf{rx}'_1 \ldots \mathbf{rx}'_\ell | \mathcal{U}_T | \mathbf{sx} + \mathbf{sx}_1 \ldots \mathbf{sx}_\ell \rangle \times |\mathbf{sx}_1 \ldots \mathbf{sx}_\ell\rangle |\mathbf{rx}'_1 \ldots \mathbf{rx}'_\ell\rangle. \tag{2.31}$$

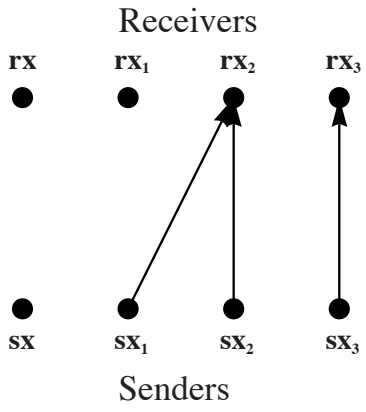

(a) A term in $|\psi_{00}\rangle$

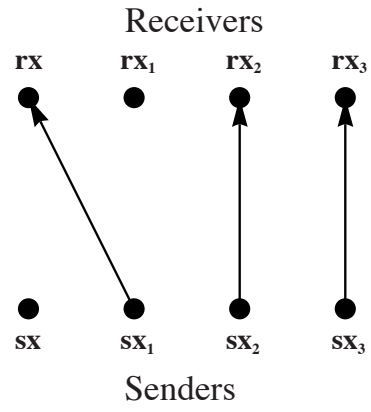

(b) A term in $|\psi_{01}\rangle$

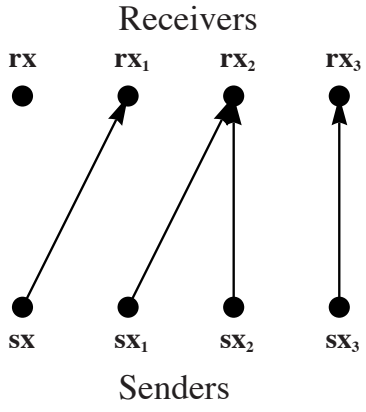

(c) A term in $|\psi_{10}\rangle$

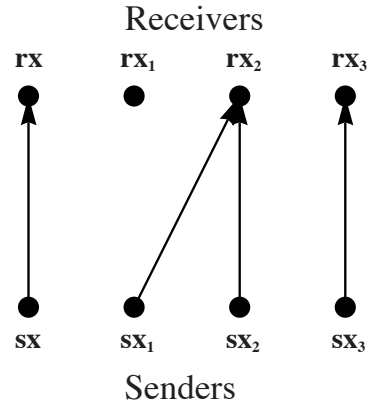

(d) A term in $|\psi_{11}\rangle$

Figure 2.5: Schematic representations of terms that contribute to the various $|\psi_{jk}\rangle$ vectors. The special pair, the pair we are focusing on, is **sx** and **rx**.

Note a subtle but important difference: this time there is no prime on the third sum. For a term to be included in $|\psi_{11}\rangle$, an excitation must have started at sender $\mathbf{sx}$, and one excitation must travel to receiver $\mathbf{rx}$, but it's perfectly fine if several excitations travel there also. If it weren't for this fact, there would be a one-to-one correspondence between terms in $|\psi_{00}\rangle$ and terms in $|\psi_{11}\rangle$. Still, we'd like to take advantage of this near correspondence, so let's write $|\psi_{11}\rangle = |\psi_{11}^{00}\rangle + |\psi_{11}^{01}\rangle$, with

$$|\psi_{11}^{00}\rangle = \frac{1}{\sqrt{2^{M-1}}} \sum_{\ell=0}^{M-1} \sum_{\{\mathbf{x}_1 \ldots \mathbf{x}_\ell\}}{}' \overline{\sum_{\{\mathbf{x}'_1 \ldots \mathbf{x}'_\ell\}}{}'} \langle \mathbf{rx} + \mathbf{rx}'_1 \ldots \mathbf{rx}'_\ell | \mathcal{U}_T | \mathbf{sx} + \mathbf{sx}_1 \ldots \mathbf{sx}_\ell \rangle \times |\mathbf{sx}_1 \ldots \mathbf{sx}_\ell\rangle |\mathbf{rx}'_1 \ldots \mathbf{rx}'_\ell\rangle \tag{2.32}$$

and

$$|\psi_{11}^{01}\rangle = \frac{1}{\sqrt{2^{M-1}}} \sum_{\ell=0}^{M-2} \sum_{\{\mathbf{x}_1 \ldots \mathbf{x}_{\ell+1}\}}{}' \overline{\sum_{\{\mathbf{x}'_1 \ldots \mathbf{x}'_\ell\}}} \langle \mathbf{rx} + \mathbf{rx} + \mathbf{rx}'_1 \ldots \mathbf{rx}'_\ell | \mathcal{U}_T | \mathbf{sx} + \mathbf{sx}_1 \ldots \mathbf{sx}_{\ell+1} \rangle \times |\mathbf{sx}_1 \ldots \mathbf{sx}_\ell\rangle |\mathbf{rx} + \mathbf{rx}'_1 \ldots \mathbf{rx}'_\ell\rangle. \tag{2.33}$$

Notice that $|\psi_{11}^{00}\rangle$ and $|\psi_{11}^{01}\rangle$ are orthogonal: $\langle \psi_{11}^{00} | \psi_{11}^{01} \rangle = 0$, and that there really is a one-to-one correspondence between terms in $|\psi_{00}\rangle$ and terms $|\psi_{11}^{00}\rangle$. Moreover, in the weak coupling regime ($\eta \ll 1$) the two vectors are very nearly parallel. From the form of $\mathbb{K}$ in (2.23), one finds that at the transfer time T,

$$|\langle \mathbf{rx} | \mathbb{K}^\dagger | \mathbf{sx} \rangle_{\mathcal{G}}| = 1 - \frac{1}{2}\eta^2 m \sin^2 \xi_T + O(\eta^3) \tag{2.34}$$

and

$$|\langle \mathbf{rx} | \mathbb{K}^\dagger | \mathbf{sx}' \rangle_{\mathcal{G}}| = \eta |\sin \xi_T| + O(\eta^2). \tag{2.35}$$

Now, consider the matrix elements $\langle \mathbf{rx} + \mathbf{rx}_1 \ldots \mathbf{rx}_\ell | \mathcal{U}_T | \mathbf{sx} + \mathbf{sx}_1 \ldots \mathbf{ss}_\ell \rangle$ which appear in (2.32). Because all of the $\mathbf{rx}_j$'s are distinct from $\mathbf{rx}$, we can use the permanent formula (2.12) for ℓ-excitation subspace matrix elements of $\mathcal{U}_t$ together with (2.34) and (2.35) to conclude that

$$\langle \mathbf{rx} + \mathbf{rx}'_1 \ldots \mathbf{rx}'_\ell | \mathcal{U}_T | \mathbf{sx} + \mathbf{sx}_1 \ldots \mathbf{sx}_\ell \rangle = \langle \mathbf{rx} | \mathcal{U}_T | \mathbf{sx} \rangle \langle \mathbf{rx}'_1 \ldots \mathbf{rx}'_\ell | \mathcal{U}_T | \mathbf{sx}_1 \ldots \mathbf{sx}_\ell \rangle + O(\eta^2). \tag{2.36}$$

Hence,

$$|\psi_{11}^{00}\rangle = \langle \mathbf{rx} | \mathcal{U}_T | \mathbf{sx} \rangle |\psi_{00}\rangle + |\varepsilon'\rangle, \tag{2.37}$$

with $\langle \varepsilon' | \varepsilon' \rangle = O(\eta^4)$. Since $|\langle \mathbf{rx} | U | \mathbf{sx} \rangle| = 1 - O(\eta^2)$, we can absorb its deviation from unity into $|\varepsilon'\rangle$,

$$|\psi_{11}^{00}\rangle = \frac{\langle \mathbf{rx} | \mathcal{U}_T | \mathbf{sx} \rangle}{|\langle \mathbf{rx} | \mathcal{U}_T | \mathbf{sx} \rangle|} |\psi_{00}\rangle + |\varepsilon\rangle, \tag{2.38}$$

and $\langle\varepsilon|\varepsilon\rangle = O(\eta^4)$ is still satisfied.

Finally, we can write the vectors $|\psi_{01}\rangle$ and $|\psi_{10}\rangle$ as

$$|\psi_{01}\rangle = \frac{1}{\sqrt{2^M}} \sum_{\ell=0}^{M-2} \sum_{\{\mathbf{x}_1 \ldots \mathbf{x}_{\ell+1}\}}{}' \overline{\sum_{\{\mathbf{x}'_1 \ldots \mathbf{x}'_\ell\}}} \langle \mathbf{rx} + \mathbf{rx}'_1 \ldots \mathbf{rx}'_\ell | \mathcal{U}_T | \mathbf{sx}_1 \ldots \mathbf{sx}_{\ell+1} \rangle \times |\mathbf{sx}_1 \ldots \mathbf{sx}_{\ell+1}\rangle |\mathbf{rx}'_1 \ldots \mathbf{rx}'_\ell\rangle \tag{2.39}$$

and

$$|\psi_{10}\rangle = \frac{1}{\sqrt{2^M}} \sum_{\ell=0}^{M-1} \sum_{\{\mathbf{x}_1 \ldots \mathbf{x}_\ell\}}{}' \overline{\sum_{\{\mathbf{x}'_1 \ldots \mathbf{x}'_{\ell+1}\}}{}'} \langle \mathbf{rx}'_1 \ldots \mathbf{rx}'_{\ell+1} | \mathcal{U}_T | \mathbf{sx} + \mathbf{sx}_1 \ldots \mathbf{sx}_\ell \rangle \times |\mathbf{sx} + \mathbf{sx}_1 \ldots \mathbf{sx}_\ell\rangle |\mathbf{rx}'_1 \ldots \mathbf{rx}'_{\ell+1}\rangle. \tag{2.40}$$

Notice the one-to-one correspondence between terms in $|\psi_{01}\rangle$ and the terms in $|\psi_{11}^{01}\rangle$ (hence our choice for its name). In fact, these two vectors are also very nearly parallel.

Finally, we point out a fact that will be very helpful in just a moment, when we need to calculate $\langle\psi_{jk}|\psi_{jk}\rangle$: in a given $|\psi_{jk}\rangle$ vector, all terms are orthogonal. This is because excitations on the Receivers' Cube, which would usually be indistinguishable, are distinguished by the state of the senders' auxiliary qubits.

Bounding the Fidelity

The state of the system at time T can be written as

$$\begin{aligned} |\mathrm{system}(T)\rangle =& \frac{1}{\sqrt{2}}\Big(|00\rangle|\psi_{00}\rangle + e^{2i\varphi}|11\rangle|\psi_{00}\rangle\Big) + \frac{1}{\sqrt{2}}\Big(|11\rangle|\psi_{11}^{01}\rangle + |11\rangle|\varepsilon\rangle\Big) \\ &+ |01\rangle|\psi_{01}\rangle + |10\rangle|\psi_{10}\rangle, \end{aligned} \tag{2.41}$$

with $e^{2i\varphi} = \frac{\langle \mathbf{rx}|U|\mathbf{sx}\rangle}{|\langle \mathbf{rx}|U|\mathbf{sx}\rangle|}$. By each applying the local unitary $U_\varphi = \left(\begin{smallmatrix} 1 & 0 \\ 0 & e^{-i\varphi} \end{smallmatrix}\right)$ to their qubits, sender $\mathbf{sx}$ and receiver $\mathbf{rx}$ can transform the system into the state

$$\begin{aligned} |\widetilde{\mathrm{system}}(T)\rangle =& \frac{1}{\sqrt{2}}\Big(|00\rangle|\psi_{00}\rangle + |11\rangle|\psi_{00}\rangle\Big) + \frac{e^{-2i\varphi}}{\sqrt{2}}\Big(|11\rangle|\psi_{11}^{01}\rangle + |11\rangle|\varepsilon\rangle\Big) \\ &+ e^{-i\varphi}|01\rangle|\psi_{01}\rangle + e^{-i\varphi}|10\rangle|\psi_{10}\rangle. \end{aligned} \tag{2.42}$$

Now, the fidelity of the transfer is given by $F_{\mathbf{sx}\to\mathbf{rx}} = \langle\Phi^+|\widetilde{\rho}_{A_\mathbf{x}B_\mathbf{x}}(T)|\Phi^+\rangle$, where $\widetilde{\rho}_{A_\mathbf{x}B_\mathbf{x}}$ is the reduced density matrix for the pair of qubits possessed by sender $\mathbf{sx}$ and receiver $\mathbf{rx}$. However, we can put a lower bound on the fidelity by taking $|\langle\Phi^+|\langle\psi|\widetilde{\mathrm{system}}(T)\rangle|^2$, where $|\psi\rangle$ is some state of the oscillator network and the other senders' qubits. In particular, using $|\psi\rangle = \frac{|\psi_{00}\rangle}{\sqrt{\langle\psi_{00}|\psi_{00}\rangle}}$,

$$F_{\mathbf{sx}\to\mathbf{rx}}^{00} = \frac{1}{\langle\psi_{00}|\psi_{00}\rangle} |\langle\Phi^+|\langle\psi_{00}|\widetilde{\mathrm{system}}(T)\rangle|^2 \tag{2.43}$$

is guaranteed to be a lower bound on the fidelity $F_{\mathbf{sx}\to\mathbf{rx}}$, and in light of the form of $|\widetilde{\text{system}}(T)\rangle$ in (2.42), we expect this lower bound to be rather good. We now turn to calculating $F^{00}_{\mathbf{sx}\to\mathbf{rx}}$ to second order in the coupling parameter η.

Exploiting the orthogonality of $|\psi^{01}_{11}\rangle$ and $|\psi^{00}_{11}\rangle$, and the fact that $|\langle\psi_{00}|\varepsilon\rangle|^2 \leq \langle\psi_{00}|\psi_{00}\rangle\langle\varepsilon|\varepsilon\rangle = O(\eta^4)$ (Cauchy-Schwarz inequality), one finds that

$$F^{00}_{\mathbf{sx}\to\mathbf{rx}} = \langle\psi_{00}|\psi_{00}\rangle + \frac{1}{2}\Big(e^{-2i\varphi}\langle\psi_{00}|\varepsilon\rangle + e^{2i\varphi}\langle\varepsilon|\psi_{00}\rangle\Big). \tag{2.44}$$

Using the normalization condition on $|\text{system}(T)\rangle$, (2.44) can be recast as

$$F^{00}_{\mathbf{sx}\to\mathbf{rx}} = 1 - \Big(\langle\psi_{01}|\psi_{01}\rangle + \langle\psi_{10}|\psi_{10}\rangle + \frac{1}{2}\langle\psi^{01}_{11}|\psi^{01}_{11}\rangle\Big), \tag{2.45}$$

which is much easier to deal with: each of these terms represents an error, each vector is small, and the corresponding inner product is even smaller. If we want $F^{00}_{\mathbf{sx}\to\mathbf{rx}}$ to second order in η, we need only keep track of the vectors that appear in (2.45) to first order in η.

We begin by calculating $\langle\psi_{10}|\psi_{10}\rangle$. Consider that only terms which represent a single error (a single "hop" from one channel to another) will contribute to $|\psi_{10}\rangle$ to first order in η. Further, because this is $|\psi_{10}\rangle$, an excitation must start at sender $\mathbf{sx}$, and it must hop to another channel. Thus, every other excitation must make it to its corresponding receiver in order for a term to contribute to $\langle\psi_{10}|\psi_{10}\rangle$. Moreover, because every term is orthogonal to every other term (since they are distinguished by the senders' qubits), we have that

$$\langle\psi_{10}|\psi_{10}\rangle = \frac{1}{2^M}\sum_{\ell=0}^{M-1}\sum_{\{\mathbf{x}_1\ldots\mathbf{x}_\ell\}}{}'\sum_{\substack{\mathbf{x}'\\ d_H(\mathbf{x},\mathbf{x}')=1}} |\langle\mathbf{rx}'+\mathbf{rx}_1\ldots\mathbf{rx}_\ell|\mathcal{U}_T|\mathbf{sx}+\mathbf{sx}_1\ldots\mathbf{sx}_\ell\rangle|^2, \tag{2.46}$$

where the third sum is over bitstrings $\mathbf{x}'$ a Hamming distance 1 from $\mathbf{x}$, i.e. over channels adjacent to $C_{\mathbf{x}}$. Using (2.12), the matrix element $\langle\mathbf{rx}'+\mathbf{rx}_1\ldots\mathbf{rx}_\ell|\mathcal{U}_T|\mathbf{sx}+\mathbf{sx}_1\ldots\mathbf{sx}_\ell\rangle$ can be written as a sum of products of matrix elements of the mode evolution operator $\mathbb{K}$. Of these, only the main term, in which $\mathbf{sx}_j$ is paired with $\mathbf{rx}_j$ for all j, contributes. Since $|\langle\mathbf{rx}_j|\mathbb{K}^\dagger|\mathbf{sx}_j\rangle_{\mathcal{G}}| = 1$ and $|\langle\mathbf{rx}'|\mathcal{U}_T|\mathbf{sx}\rangle| = \eta|\sin\xi_T|$ to first order in η, we have

$$|\langle\mathbf{rx}'+\mathbf{rx}_1\ldots\mathbf{rx}_\ell|\mathcal{U}_T|\mathbf{sx}+\mathbf{sx}_1\ldots\mathbf{sx}_\ell\rangle|^2 = \begin{cases} \eta^2\sin^2\xi_T & \text{if } \mathbf{x}'\notin\{\mathbf{x}_1\ldots\mathbf{x}_\ell\} \\ 2\eta^2\sin^2\xi_T & \text{if } \mathbf{x}'\in\{\mathbf{x}_1\ldots\mathbf{x}_\ell\} \end{cases}. \tag{2.47}$$

(Because the $\mathbf{x}_j$'s are all distinct, $\mathbf{x}'$ can be the same as only one of them. Hence the $p!$ in (2.12) can be only 1 or 2.)

The sum for $\langle\psi_{10}|\psi_{10}\rangle$, then, is:

$$\begin{aligned}\langle\psi_{10}|\psi_{10}\rangle =&\frac{1}{2^M}\sum_{\ell=0}^{M-1}\sum_{\{\mathbf{x}_1\ldots\mathbf{x}_\ell\}}{}'\sum_{\substack{\mathbf{x}'\notin\{\mathbf{x}_1\ldots\mathbf{x}_\ell\}\\ d_H(\mathbf{x},\mathbf{x}')=1}}\eta^2\sin^2\xi_T \;+\; 2\frac{1}{2^M}\sum_{\ell=0}^{M-1}\sum_{\{\mathbf{x}_1\ldots\mathbf{x}_\ell\}}{}'\sum_{\substack{\mathbf{x}'\in\{\mathbf{x}_1\ldots\mathbf{x}_\ell\}\\ d_H(\mathbf{x},\mathbf{x}')=1}}\eta^2\sin^2\xi_T\\ =&\frac{1}{2^M}\sum_{\ell=0}^{M-1}\sum_{\{\mathbf{x}_1\ldots\mathbf{x}_\ell\}}{}'\sum_{\substack{\mathbf{x}'\\ d_H(\mathbf{x},\mathbf{x}')=1}}\eta^2\sin^2\xi_T \;+\; \frac{1}{2^M}\sum_{\ell=0}^{M-1}\sum_{\{\mathbf{x}_1\ldots\mathbf{x}_\ell\}}{}'\sum_{\substack{\mathbf{x}'\in\{\mathbf{x}_1\ldots\mathbf{x}_\ell\}\\ d_H(\mathbf{x},\mathbf{x}')=1}}\eta^2\sin^2\xi_T\end{aligned} \tag{2.48}$$

Calculating $\langle\psi_{10}|\psi_{10}\rangle$ is now only a matter of counting the number of terms. To deal with the first sum in (2.48), first note that there are m channels adjacent to channel $\mathbf{x}$, and hence m possibilities for $\mathbf{x}'$. There are then $M-1$ remaining senders, from which we choose ℓ to start in the $|1\rangle$ state. Thus:

$$\frac{1}{2^M}\sum_{\ell=0}^{M-1}\sum_{\{\mathbf{x}_1\ldots\mathbf{x}_\ell\}}{}'\sum_{\substack{\mathbf{x}'\\ d_H(\mathbf{x},\mathbf{x}')=1}} = \frac{m}{2^M}\sum_{\ell=0}^{M-1}\binom{M-1}{\ell} = \frac{m}{2}. \tag{2.49}$$

In the second sum there are again m possibilities for $\mathbf{x}'$, but this bitstring must be a member of the set $\{\mathbf{x}_1\ldots\mathbf{x}_\ell\}$. Thus, when choosing the set $\{\mathbf{x}_1\ldots\mathbf{x}_\ell\}$, we do not choose ℓ bitstrings, we choose only $\ell-1$, *and* the set we're choosing from is all the senders, except $\mathbf{x}$ and $\mathbf{x}'$—a set of size $M-2$. Thus:

$$\frac{1}{2^M}\sum_{\ell=0}^{M-1}\sum_{\{\mathbf{x}_1\ldots\mathbf{x}_\ell\}}{}'\sum_{\substack{\mathbf{x}'\in\{\mathbf{x}_1\ldots\mathbf{x}_\ell\}\\ d_H(\mathbf{x},\mathbf{x}')=1}} = \frac{m}{2^M}\sum_{\ell=0}^{M-2}\binom{M-2}{\ell} = \frac{m}{4}. \tag{2.50}$$

Thus, we finally have that

$$\langle\psi_{10}|\psi_{10}\rangle = 1-\frac{3}{4}m\eta^2\sin^2\xi_T. \tag{2.51}$$

Now consider $\langle\psi_{01}|\psi_{01}\rangle$, which represent terms in which sender $\mathbf{sx}$ starts in the $|0\rangle$ state, but an excitation leaks onto channel $\mathbf{x}$:

$$\langle\psi_{01}|\psi_{01}\rangle = \frac{1}{2^M}\sum_{\ell=0}^{M-2}\sum_{\{\mathbf{x}_1\ldots\mathbf{x}_{\ell+1}\}}{}'\overline{\sum_{\{\mathbf{x}'_1\ldots\mathbf{x}'_\ell\}}}|\langle\mathbf{rx}+\mathbf{rx}'_1\ldots\mathbf{rx}'_\ell|\mathcal{U}_T|\mathbf{sx}_1\ldots\mathbf{sx}_{\ell+1}\rangle|^2 \tag{2.52}$$

Again, the excitation that leaks onto channel $\mathbf{x}$ must come from an adjacent channel, and every other sender's excitation must go to the corresponding receiver. Thus:

$$\langle\psi_{01}|\psi_{01}\rangle = \frac{1}{2^M}\sum_{\ell=0}^{M-1}\sum_{\{\mathbf{x}_1\ldots\mathbf{x}_\ell\}}{}'\sum_{\substack{\mathbf{x}'\notin\{\mathbf{x}_1\ldots\mathbf{x}_\ell\}\\ d_H(\mathbf{x},\mathbf{x}')=1}}|\langle\mathbf{rx}+\mathbf{rx}_1\ldots\mathbf{rx}_\ell|\mathcal{U}_T|\mathbf{sx}'+\mathbf{sx}_1\ldots\mathbf{sx}_\ell\rangle|^2, \tag{2.53}$$

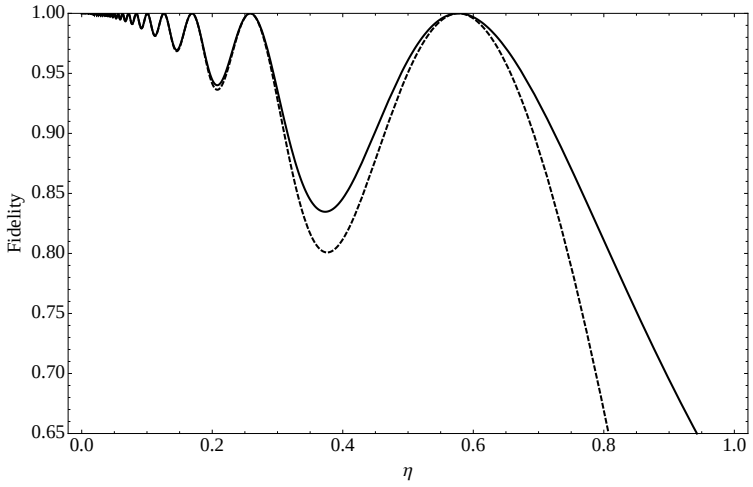

Figure 2.6: The fidelity of the entanglement transfer is bounded from below by $F^{00}_{\mathbf{sx}}$ (solid), which is plotted, along with its approximation (dashed) for $m = 1$.

here $\mathbf{sx}'$ is the sender adjacent to $\mathbf{sx}$ whose excitation ends up at $\mathbf{rx}$. Because $\mathbf{x}_1$ through $\mathbf{x}_\ell$ are all different, and none of them is $\mathbf{x}$, the matrix elements in (2.53) are always $\eta^2 \sin^2 \xi_T$. There are m choices for $\mathbf{sx}'$, and then there are ℓ remaining other senders to pick from a set of $M - 2$, so

$$\langle \psi_{01} | \psi_{01} \rangle = \frac{m}{2^M} \sum_{\ell=0}^{M-2} \binom{M-2}{\ell} \eta^2 \sin^2 \xi_T = \frac{m}{4} \eta^2 \sin^2 \xi_T. \tag{2.54}$$

The arguments are all the same for $\langle \psi^{01}_{11} | \psi^{01}_{11} \rangle$, except it has a factor of $\frac{1}{2^{M-1}}$ out front, and the matrix elements are always $2\eta^2 \sin^2 \xi_T$ because when an excitation leaks onto channel $\mathbf{x}$, there was already an excitation there already. Thus:

$$\langle \psi^{01}_{11} | \psi^{01}_{11} \rangle = 2 \frac{m}{2^{M-1}} \sum_{\ell=0}^{M-2} \binom{M-2}{\ell} \eta^2 \sin^2 \xi_T = m \eta^2 \sin^2 \xi_T. \tag{2.55}$$

Writing $m = \log_2 M$, we finally have as our lower bound

$$\boxed{F^{00}_{\mathbf{sx}\to\mathbf{rx}} = 1 - (\log_2 M)\, \eta^2 \sin^2 \xi_T} \qquad \text{(Second order in } \eta) \tag{2.56}$$

which is independent of the sender $\mathbf{sx}$. Thus, each and every sender can achieve entanglement transfer with a fidelity bounded from below by (2.56): the error in the transfer scales no quicker than as the logarithm of the number of senders using the network. Figure 2.6 shows $F^{00}_{\mathbf{sx}\to\mathbf{rx}}$ and the approximation (2.56) for $m = 1$. We can identify two types of errors that cause the fidelity to deviate from unity: excitations leaking off of channel $\mathbf{sx}$ (represented by $\langle \psi_{10} | \psi_{10} \rangle$), and excitations leaking onto channel $\mathbf{sx}$ (represented by $\langle \psi_{01} | \psi_{01}$ and $\frac{1}{2} \langle \psi^{01}_{11} | \psi^{01}_{11} \rangle$). In the case discussed here, these two types of errors contribute equally, each reducing the fidelity by $\frac{3}{4} m \eta^2 \sin^2 \xi_T$.

While the results of this section are specific to hypercube networks split according to the $\Omega^{(\text{diag})}$ of (2.17), the methods used to derive (2.56) seem general. We thus conjecture that the error in the fidelity of parallel entanglement distribution on a network split into weakly coupled channels will, for a particular channel $C_{\mathbf{x}}$, scale as $m\eta^2$ where η is the coupling constant and m is the number of channels adjacent to $C_{\mathbf{x}}$.

2.4 Oscillator vs. Spins: A Hypercube Comparison

2.4.1 A Qubit-Compatible Protocol

We have seen that parallel entanglement transfer works remarkably well on oscillator networks. As noted in Section 2.2.3, the many-excitation subspace dynamics of spin networks are considerably more complicated, thwarting our attempts at significant analytical results. However, numerical evidence suggests that parallel entanglement distribution on hypercube spin networks is similar to distribution on hypercube oscillator networks, with some important differences.

Consider trying to transfer entanglement in parallel on a hypercube spin network in exactly the same manner as described in Section 2.3: again, the cube is split into 2^m channels effectively decoupled by the same $\Omega^{(\text{diag})}$ matrix; again there is only one sender and one receiver per channel; and again the senders and receivers each form a Senders' Cube and a Receivers' Cube, so that all entanglement is being sent "in the same direction".

Figure 2.7 shows the entanglement fidelity for one of the two sender-receiver pairs in this situation, for $m = 1$ (two channels) and $d = 2$ through 6, as well as the lower bound $F^{00}_{\mathbf{sx}}$ for the oscillator case (exact, not approximate). To be clear: what is plotted for the spin network is the actual fidelity of the transfer, not some lower bound; this is a minor point, and does not affect the comparisons we make.

While the curves are qualitatively similar, there are several striking differences. First and foremost: for $m = 1$, the spin networks seem to do better on average, but they fail to achieve perfect state transfer. They do exhibit the same oscillations that the oscillator curve does, but they fail to reach unity. However, analytic investigations for $d = 2$ and $d = 3$ show that if η makes the error in the oscillator fidelity vanish, it also makes the second order error in the fidelity for qubit networks vanish. That qubit networks do better on average can be explained qualitatively as follows: while on oscillator networks an excitation could always leak to an adjacent channel, the presence of an excitation on an adjacent channel in the qubit network prevents the hopping in this case[4]. The qubits behave somewhat like hard-core bosons.

[4]If we were to consider two senders and two receivers using a hypercube of spins but transferring entanglement in opposite directions, we would observe that the fidelity is lower because there wouldn't be an excitation on the adjacent channel to act as a "plug". In contrast, performing the transfer in opposing directions actually *increases* the fidelity on oscillator networks, because then, while sender **sx**'s excitation can leak out of her channel, other excitations won't leak in.

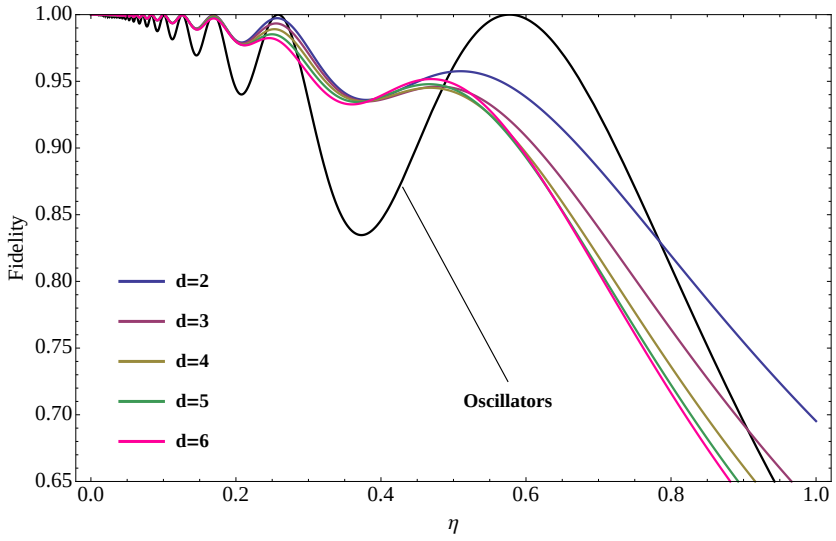

Figure 2.7: The fidelity of entanglement transfer for a d-dimensional hypercube network of spins split into two channels with one sender and receiver per channel, with entanglement being sent in the same direction on each channel for $d = 2$ through 6. Shown also is the lower bound $F^{00}_{\mathbf{sx}}$ for the corresponding entanglement transfer on the d-dimensional hypercube oscillator network of arbitrary dimension.

Secondly, note that while the spin network fidelities behave in the same way for all d if $\eta \ll 1$, they do not for large η. In contrast, the oscillator fidelity does not depend on d at all, only on m. This follows from the fact that on oscillator networks, the bosonic excitations are all localized on the Receivers' Cube at time T. This isn't so for the spin networks, though, which means that the fidelity is sensitive to the structure of the channels themselves, in addition to how the channels are arranged.

2.4.2 A Massively Parallel Protocol

If only a single sender is transferring entanglement per channel, we have some evidence that qubit networks and oscillator networks behave qualitatively similarly. Hypercube oscillator networks, however, have a capability for routing quantum information that no qubit network could hope mimic: the capacity for what we shall call *massively* parallel entanglement distribution.

In Section (2.3) we broke the d-dimensional cube into subcube channels $C_{\mathbf{x}} = \{\mathbf{yx}|\mathbf{y} \in \mathbb{Z}_2^{(d-m)}\}$, and calculated the fidelity for $00\ldots00\mathbf{x}$ to transfer half a Bell state $|\Phi^+\rangle$ to the antipodal vertex on that channel, $11\ldots11\mathbf{x}$. There was only a single sender and receiver per channel. What if *every* vertex on the entire network acted as a sender, with vertex $\mathbf{yx}$ trying to transfer half a Bell pair to vertex $\overline{\mathbf{y}}\mathbf{x}$? If done faithfully, this would be true massively parallel entanglement transfer, as illustrated in Fig. 2.8. However, we already have a lower bound on the fidelity for this massively parallel transfer for sender $\mathbf{yx}$—$F^{00}_{\mathbf{sx}\to\mathbf{rx}}$! Because the excitations due to all the senders

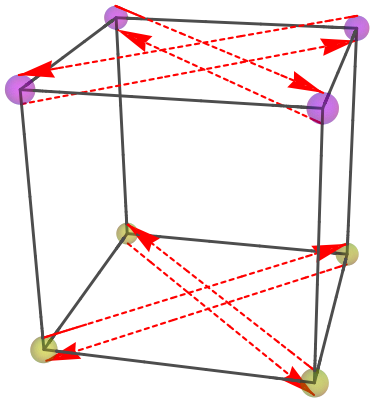

Figure 2.8: Massively-parallel entanglement transfer for $d = 3$, here with $M = 2$ channels.

in the set

$$S_{\mathbf{y}} = \{\mathbf{yx}|\mathbf{x} \in \mathbb{Z}_2^m\} \tag{2.57}$$

are localized on the vertices in the set $S_{\overline{\mathbf{y}}}$, our earlier analysis applies. The excitations within the oscillator network just "pass through" other, behaving as noninteracting phonons.

No qubit network could ever hope to exhibit this capacity for massively parallel entanglement transfer because it requires the excitations to pass through each other by exploring oscillator levels beyond $|0\rangle$ and $|1\rangle$.

In the next chapter, we'll see that both the qubit-compatible protocol and the massively parallel protocol can distribute entanglement much more efficiently than single-user (serial) protocols.

Chapter 3

Entanglement Distribution Schemes

3.1 Efficiency

Imagine building a quantum computer in which quantum communication between registers is based upon teleportation, and entangled pairs are distributed by an oscillator network with network graph $\mathcal{G}$. Let us assume that every register needs to be capable of sending quantum information to every other register. One possible way to achieve this is to have every register share entangled qubit pairs with every other register[1].

In this chapter we assess the effectiveness of d-dimensional hypercube networks at distributing entanglement between each pair of nodes. We assume the following three "rules":

1. All network couplings are equal to Ω_0.

2. The oscillator that make up the network have programmable energy levels: the operators of the quantum computer have complete control over them, and they can be changed from one use of the network to another.

3. Each node can generate maximally entangled pairs of qubits.

For a particular entanglement distribution scheme we define the *distribution time* T_D to be the time required to distribute an approximate Bell pair between every pair of nodes. We quantify the efficiency of the distribution scheme by the distribution rate $\mathcal{R}$, given by

$$\mathcal{R} = \frac{1}{T_D} \sum_{\text{pairs } \{u,\, v\}} F_{u \to v}, \tag{3.1}$$

[1]This isn't the only way, or necessarily the best. Every register could, for example, share entangled pairs with a hub. Then if register u wanted to send a state to register v, it could first send the state to the hub, and then the hub could send the state to register v.

where $F_{u\to v}$ is the fidelity of the entanglement transfer when vertex u acts as sender and vertex v acts as receiver. The rate $\mathcal{R}$ is the number of approximate Bell pairs distributed per unit time, weighted by their fidelities.

Consider the case depicted in Figure 3.1: distributing entangled pairs in a quantum computer with four registers connected by a square oscillator network. The distribution could be achieved by using the qubit-compatible entanglement transfer protocol of Section 2.3 several times. State transfer is performed twice on the symmetric square (1-channel square), and once on each of the two possible 2-channel squares. Figure 3.1 shows the necessary decompositions of the square into channels. The network is used four times, and in each use the transfer time is T. The oscillator energies are reprogrammed twice, but we will always assume that this takes a time small in comparison with the transfer time T. The distribution time, then, is $4T$. Entanglement transfer is achieved twice with perfect fidelity, and four times with a fidelity of $1-\frac{3}{2}\eta^2\sin^2\xi_T$. The efficiency of the square network using qubit-compatible distribution, then, is:

$$\begin{aligned}\mathcal{R} =& \frac{1+1+4(1-\frac{3}{2}\eta^2\sin^2\xi_T)}{4T}\\ =& \frac{1}{T}\frac{3}{2}\left(1-\eta^2\sin^2\xi_T\right)\end{aligned} \tag{3.2}$$

3.1.1 Distillable Entanglement Revisited

Just as the proper way to quantify the entanglement transferred from sender to receiver is not by the fidelity of the transfer, but by the bits of distillable entanglement transferred, a better way to quantify the efficiency of an entanglement distribution scheme would be by the rate of distillable entanglement transferred:

$$\mathcal{R}^{(\text{better})} = \frac{\text{bits of distillable entanglement transferred between all nodes}}{\text{distribution time}}. \tag{3.3}$$

After n rounds of the entanglement distribution scheme have been performed, there would really be $n\mathcal{R}^{(\text{better})}$ perfect Bell states shared between the nodes (with n large). Hence, $\mathcal{R}^{(\text{better})}$ would be a truly great way to quantify the the efficiency of a distribution scheme—if only it could be calculated. As noted in Section 1.3, the distillable entanglement of an arbitrary two-qubit mixed state is not even known.

As a practical matter, then, we will use $\mathcal{R}$ as defined in (3.1) to quantify efficiency. However, it is some consolation that the distillation method proposed by Bennett et. al. (Section 1.3.3, or [19]) is a convex[2] function of the fidelity. Thus, a lower bound on the $\mathcal{R}$ can be used to put a lower bound on $\mathcal{R}^{(\text{better})}$ via their distillation method.

[2]A function $f : X \to \mathbb{R}$ is said to be convex if $f(\frac{\rho+\sigma}{2}) < \frac{f(\rho)+f(\sigma)}{2}$ for all $\rho, \sigma \in X$. It should be mentioned that the distillable entanglement itself is thought *not* to be a convex function of the density matrix [23].

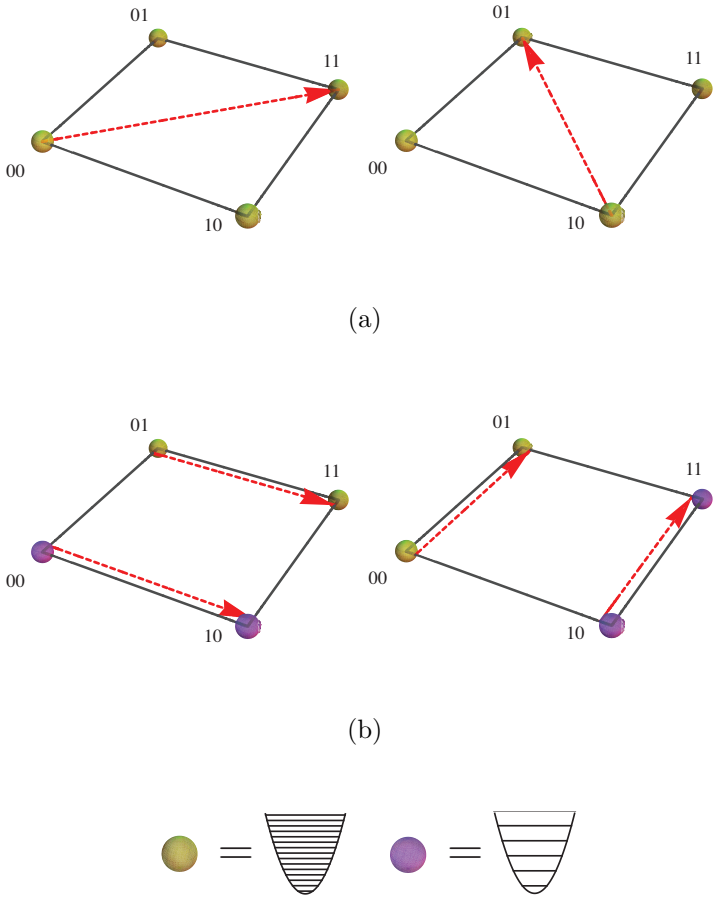

Figure 3.1: Entanglement distribution on a quantum computer with four registers connected in a square network. **(a)**: The network is used twice to by a single user. **(b)**: Two 2-channel configurations are used. Each configuration is used once by two senders simultaneously.

3.2 Efficiency of Hypercube Networks

We now turn to calculating the efficiency of the d-dimensional hypercube networks. We compare three schemes for distributing entanglement. First, we briefly consider the efficiency of distribution if only one vertex is allowed to send entanglement at a time: this is the single-user, or serial, distribution scheme. Second, we consider the qubit-compatible scheme that we focused on in Section 2.3. Finally, we analyze the dream-scheme: the massively-parallel protocol mentioned in Section 2.4.2.

3.2.1 Single-User Distribution

In single-user (SU) distribution, the oscillators of the d-dimensional hypercube are split into two categories: channel and non-channel. If the sender and receiver are on vertices a Hamming distance m apart, they *define* an m-dimensional subcube, with themselves as antipodal vertices of the subcube. We have seen that faithful state transfer is possible from corner to corner of such a channel in time $T = \frac{\pi}{2\Omega_0}$, independent of channel size. This case is more interesting as a comparison with other cases than in its own right. It is sufficient for this purpose to say that the fidelity cannot be greater than unity, and since only one sender uses the network at a time, the transfer rate is bounded from above by:

$$\mathcal{R}^{(\mathrm{SU})} \leq \frac{1}{T}. \tag{3.4}$$

3.2.2 Qubit-Compatible Distribution

Qubit-compatible (QC) distribution was extensively discussed in Section 2.3 and allows 2^m senders to transfer entanglement simultaneously. In this scheme the hypercube is split into the 2^m channels,

$$C_{\mathbf{x}} = \{\mathbf{yx} | \mathbf{y} \in \mathbb{Z}_2^{(d-m)}\}. \tag{3.5}$$

This splitting is achieved by detuning the oscillator energies of adjacent channels from one another. In particular, oscillators on channel $C_{\mathbf{x}}$ have energy level splittings given by

$$\Omega_{\mathbf{yx},\mathbf{yx}} = \frac{\Delta\omega}{2}(1 - 2w_H(\mathbf{x})). \tag{3.6}$$

(C.f. (2.17)—this is equivalent). The dimensionless parameter $\eta = \frac{2\Omega_0}{\Delta\omega}$ quantifies the coupling between adjacent channels.

The main result of Chapter 2 was that every sender in the set

$$S_{\mathbf{y}} = \{\mathbf{yx} | \mathbf{x} \in Z_2^m\} \tag{3.7}$$

can transfer half of the bell state $|\Phi^+\rangle = \frac{1}{\sqrt{2}}(|00\rangle + |11\rangle)$ to the corresponding member of the set $S_{\overline{\mathbf{y}}}$ in a time $T = \frac{\pi}{2\Omega_0}$ with fidelity

$$F_{\mathbf{yx}\to\overline{\mathbf{y}}\mathbf{x}} \gtrsim 1 - \frac{3}{2}m\eta^2 \sin\xi_T, \tag{3.8}$$

with $\xi_T = \frac{\pi}{2}\sqrt{1+\eta^{-2}}$. We use the symbol "$\gtrsim$" here to mean that the right-hand-side is correct as a lower bound of the left to second order in η (at least for $m = 1$ it is a true lower bound; see Figure 2.6).

Bandwidth Considerations

The qubit-compatible parallel entanglement transfer scheme allows 2^m senders to transfer entanglement to receivers who are a Hamming distance $(d-m)$ away—at the other end of their respective subcube channels. To distribute approximate Bell states between every pair of nodes on a d-cube, then, requires using the qubit-compatible transfer protocol with $m = 0, 1, 2, 3 \ldots, d-1$. Generally, the operators of the quantum network can choose η to be different for each use of the network, i.e. for each value of m. In fact, we argue that if bandwidth is limited, they must do this.

Consider that when the d-cube is split into 2^m subcube channels, the oscillators that have the most closely spaced energy levels are the oscillators on channel $C_{1\ldots1}$, and the oscillators that have the farthest apart energy levels are on the channel $C_{0\ldots0}$ (see (3.6)). The difference between the energy level spacings on channel $C_{1\ldots1}$ and channel $C_{0\ldots0}$ is

$$\Omega_{1\ldots1\mathbf{x},1\ldots1\mathbf{x}} - \Omega_{0\ldots0\mathbf{x},0\ldots0\mathbf{x}} = m\Delta\omega. \tag{3.9}$$

In a real-life situation, it would probably be necessary that all of the oscillator energy level spacings $\Omega_{\mathbf{yx},\mathbf{yx}}$ lie within some bandwidth $\omega_{\max} - \omega_{\min}$. The operators of the quantum computer wish to pick the coupling η so as to make the fidelity of every transfer close to unity. A clever, but perhaps too difficult, way to achieve high fidelity transfer would be to pick η to be on resonance each time, so that the condition (2.26) for perfect state transfer is always met.

A reasonable strategy that the senders could use is to always use the maximum possible bandwidth, so that

$$\Omega_{1\ldots1\mathbf{x},1\ldots1\mathbf{x}} - \Omega_{0\ldots0\mathbf{x},0\ldots0\mathbf{x}} = \omega_{\max} - \omega_{\min}. \tag{3.10}$$

This amounts to choosing the detuning between channels, $\Delta\omega$, to be

$$\Delta\omega = \frac{\omega_{\max} - \omega_{\min}}{m}. \tag{3.11}$$

This is the strategy for choosing η that we will analyze. The fidelity of the parallel entanglement transfer for 2^m senders can then be written as

$$F_{\mathbf{yx}\to\bar{\mathbf{y}}\mathbf{x}} \gtrsim 1 - \frac{3}{2} m^3 \widetilde{\eta}^2 \sin^2 \xi_T, \tag{3.12}$$

where $\widetilde{\eta} = \frac{2\Omega_0}{\omega_{\max}-\omega_{\min}}$ is a truly m-independent coupling constant. Note that $\xi_T = \sqrt{1 + m^{-2}\widetilde{\eta}^{-2}}$, though, still carries m-dependence.

Calculating the Efficiency

Figure 3.2(a) shows the decomposition of the 3-cube into the two 2-cube channels specified by equations (3.5) and (3.6). If one's goal is to distribute entanglement between nodes that are a distance 2 apart on the 3-cube, this decomposition will help, but it won't be enough. There are two other decompositions needed, shown in

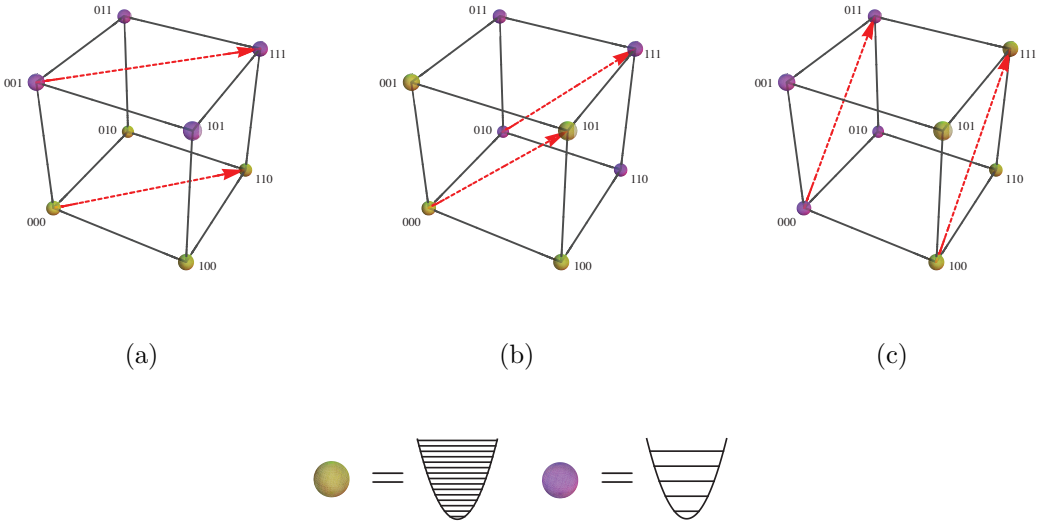

Figure 3.2: The three decompositions of the 3-cube into two 2-cube channels. We call each of these a 1-configuration, because the decompositions split the cube into 2^1 channels of dimension 2=3-1.

Figure 3.2(b) and 3.2(c). Entanglement transfer by these decompositions proceeds with the same fidelity as the first.

In general, we call each of the decompositions of the d-cube into 2^m $(d-m)$-dimensional subcube channels an *m-configuration* of the d-cube. Formally, the configuration can be thought of as the set of channels. When the operators of network set the oscillator energies Ω_{vv} to particular values, they specify a particular configuration. We have seen that the 3-cube has three 2-configurations.

A vertex is a bitstring. A channel is a set of bitstrings, which have m bits—the "fixed-bits"—all the same. A configuration is the choice of which m bits are all of the same. In Chapter 2 we dealt always with a particular configuration—the configuration in which the fixed bits were the last m bits of the bitstring. The other $(d-m)$ bits of the bitstring are "free-bits"; these label position on the channel (in Chapter 2, these always occured at the front of the bitstring). Because there are $\binom{d}{m}$ choices for the fixed-bits, there are $\binom{d}{m}$ m-configurations of the d-cube.

If $\mathbf{z}$ and $\mathbf{z}'$ are antipodal vertices of a channel in one configuration, they can't be antipodal vertices of a channel in another configuration. It follows that each configuration must be used at least once. A channel is a subcube of dimension $(d-m)$, so it has 2^{d-m-1} antipodal pairs. Each configuration must thus be used 2^{d-m-1} times. This is illustrated for each configuration of the 3-cube in Figure 3.3. Thus, the distribution time is

$$T_D^{(\mathrm{QC})} = \sum_{m=0}^{d-1} \binom{d}{m} 2^{d-m-1} = \frac{1}{2}\left(3^d - 1\right) T. \tag{3.13}$$

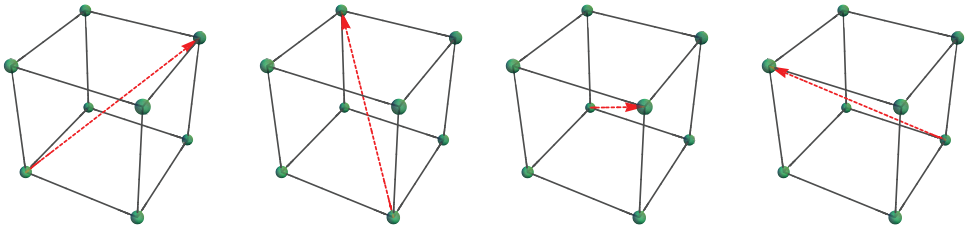

(a)

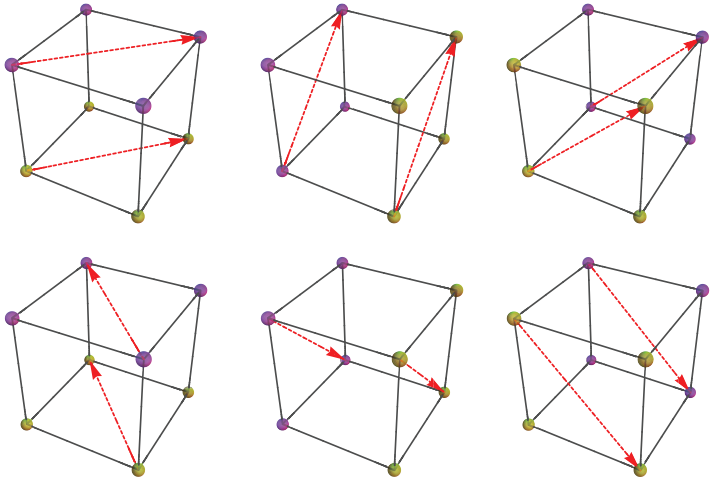

(b)

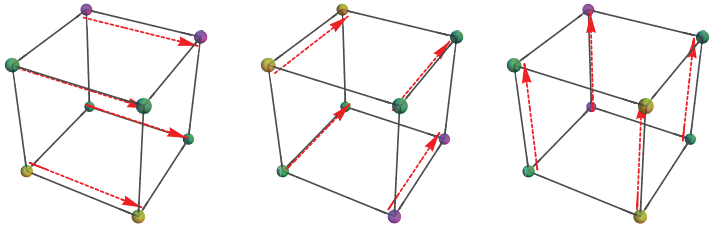

(c)

Figure 3.3: To distribute entanglement between every pair of vertices, the 3-cube network is used 13 times. **(a)**: First, no splitting is done. There is a single 3-dimensional channel that must be used four times ($m = 0$). **(b):** Next, is the $m = 1$ case. The cube is split into 2^1 subcube channels. There are three 1-cconfigurations, each of which is used twice. **(c)**: In the final, $m = 2$ case, the cube is split into 2^2 subcube channels. There are three 2-configurations, and each configuration is once only once.

During a given use, 2^m approximate Bell pair halves are transferred with fidelity bounded by (3.12). We can then write an approximate lower bound on the efficiency:

$$\mathcal{R}^{(\mathrm{QC})} \gtrsim \frac{1}{T_D^{(\mathrm{QC})}} \sum_{m=0}^{d-1} \binom{d}{m} 2^{d-1} (1 - \frac{3}{2}\widetilde{\eta}^2 m^3 \sin^2 \xi_T). \tag{3.14}$$

There is no hope of doing this sum exactly because of the m dependence of ξ_T. However, we can use the fact that $\sin^2 \xi_T \leq 1$ to write

$$\mathcal{R}^{(\mathrm{QC})} \gtrsim \frac{1}{T_D^{(\mathrm{QC})}} \sum_{m=0}^{d-1} \binom{d}{m} 2^{d-1} (1 - \frac{3}{2}\widetilde{\eta}^2 m^3). \tag{3.15}$$

This crude approximation amounts to saying that the worst case scenario is if the senders and receivers are always as far from a resonance as possible. However, the sum in (3.15) can be done. The large d behavior is:

$$\mathcal{R}^{(\mathrm{QC})} \gtrsim \frac{1}{T} N^{0.415} \left(1 - \frac{3}{16}\widetilde{\eta}^2 d^2 (d+3)\right), \tag{3.16}$$

where $N = 2^d$ is the number of nodes. (The prefactor is $(4/3)^d = N^{\log_2 \frac{4}{3}} \approx N^{0.415}$).

3.2.3 Massively-Parallel Distribution

The calculation of the massively-parallel distribution time on hypercube oscillator networks mirrors the qubit-compatible calculate. Again there are $\binom{d}{m}$ configurations. In this massively-parallel scheme, though, every vertex on the entire d-cube acts as a sender, as shown in Fig. 2.8 . Thus, each configuration needs to be used only once. The distribution time, then, is

$$T_D^{(\mathrm{MP})} = \sum_{m=0}^{d-1} \binom{d}{m} = \left(2^d - 1\right) T. \tag{3.17}$$

The numerator of the efficiency is almost the same, but the massively-parallel scheme gets an extra factor of 2: as vertex $\mathbf{z}$ sends entanglement to vertex $\mathbf{z}'$, vertex $\mathbf{z}'$ sends entanglement to $\mathbf{z}$, too. The effiency, then, is

$$\mathcal{R}^{(\mathrm{MP})} \gtrsim \frac{1}{T_D^{(\mathrm{MP})}} \sum_{m=0}^{d-1} \binom{d}{m} 2^{d} (1 - \frac{3}{2} m^3 \widetilde{\eta}^2 \sin^2 \xi_T). \tag{3.18}$$

Again, we crudely approximate $\sin^2 \xi_T = 1$. The large d behavior is, in terms of the number of nodes,

$$\mathcal{R}^{(\mathrm{MP})} \gtrsim \frac{1}{T} N \left(1 - \frac{3}{16}\widetilde{\eta}^2 d^2 (d+3)\right), \tag{3.19}$$

The massively-parallel scheme is more than quadratically better than the qubit-compatible scheme.

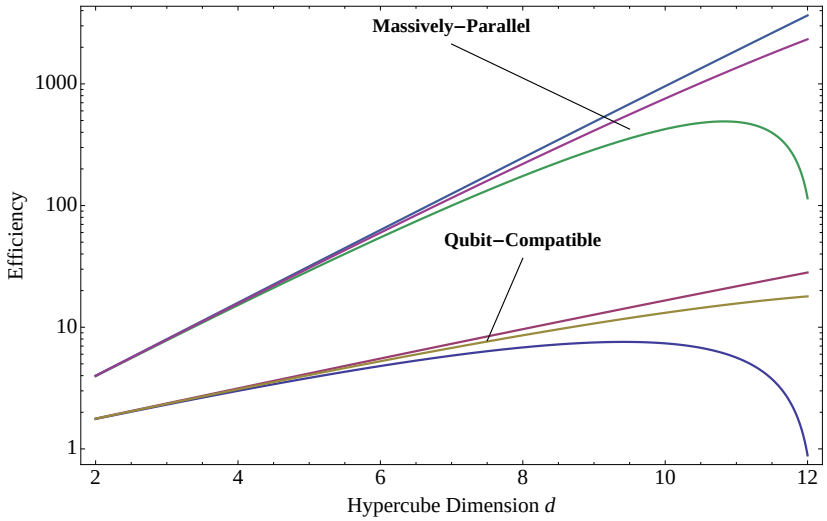

Figure 3.4: A comparison of the qubit-compatible and massively-parallel entanglement distribution rates on hypercube networks with $\widetilde{\eta} = 0.01$, $\widetilde{\eta} = 0.02$, and $\widetilde{\eta} = 0.03$.

3.2.4 Comparing the Schemes

Figure 3.4 shows a plot of the efficiency $\mathcal{R}$ for the qubit-compatible scheme and massively-parallel schemes as a function of of the dimension of the hypercube network for $\widetilde{\eta} = 0.03$, a small coupling factor. Assuming this value of $\widetilde{\eta}$, a quantum computer with 2^{10} registers connected by an oscillator network in an hypercube architecture (a Quantum Connection Machine!) could distribute entanglement 14 times faster by the qubit-compatible method than by the single-user method. If the massively-parallel method could be implemented, it would be over 800 times more efficient than the single user method.

Chapter 4

Conclusions

Efficiently routing quantum information on short distance scales is one of many key challenges that must be met before any useful quantum computer is realized.

Our results show that oscillator networks with equal couplings but programmable on-site energies can be designed to effectively and faithfully achieve parallel entanglement transfer. We considered two schemes for parallel entanglement transfer on oscillator hypercube networks: qubit-compatible transfer and massively-parallel transfer. In both schemes the hypercube is split into $M = 2^m$ effectively decoupled channels by detuning the oscillators on adjacent one channel from the oscillators on all adjacent channels. In the qubit-compatible scheme, only one sender-receiver pair uses each channel at a given time. In the massively-parallel scheme, *every* node of the network acts as a sender. In both cases the transfer has fidelity bounded from below by

$$F \gtrsim 1 - \frac{3}{2} m \eta^2 \sin^2 \xi_T, \tag{4.1}$$

where η is the effective coupling parameter and $\xi_T = \frac{\pi}{2}\sqrt{1+\eta^{-2}}$. Truly perfect state entanglement transfer occurs (for each sender) if η satisfies

$$\eta = \frac{1}{\sqrt{4n^2 - 1}} \tag{4.2}$$

for some integer n. We presented limited numerical evidence that, if the the qubit-compatible protocol were performed on a network of qubits (a spin network), the fidelity would behave qualitatively similar. Qubit networks exhibit the same resonances in the fidelity, however the fidelity is only approximately perfect when the condition (4.2) is met: for qubits, there are still fourth order deviations from unity. Massively-parallel protocols, though, cannot be achieved with qubits: they require network excitations to "pass through" each other.

Not only is faithful parallel entanglement transfer possible, but entanglement distribution schemes based upon the qubit-compaitble and massively-parallel protocols are vastly more efficient than entanglement distribution schemes in which only a single user can send entanglement at a time. In the limited case when coupling is negligible, the rate of entanglement distribution on a d-dimensional hypercube network in which the qubit-compatible protocol is used is given by $\mathcal{R}^{(\mathrm{QC})} = \frac{1}{T} N^{0.415}$, where $N = 2^d$

is the number of nodes. The corresponding limiting rate for the massively-parallel protocol is $\mathcal{R}^{(\mathrm{MP})} = \frac{1}{T}N$, which is essentially optimal.

These distribution rates are both much faster than the best rate $\mathcal{R}^{(\mathrm{SU})} = \frac{1}{T}$ possible for any single-user protocol. The efficiency of the massively-parallel distribution scheme, in particular, is breathtaking. However, it has a serious drawback: it relies on oscillators. We argued that the qubit-compatible protocol could work similarly with a qubit network; the massively-parallel protocol has no hope of working with qubit network. In practice, it may be harder to build an oscillator network because using an oscillator network to distribute entangled pairs within a qubit-based quantum computer requires a special interface between the registers of the quantum computer and the network itself. Experimental work with oscillators, though, is advancing. For several years, microwave resonators (whose modes are oscillators) have been used to couple superconducting qubits together [3, 4]. More recently, an interface between superconducting qubits and microwave resonators of the type that would be necessary in a quantum computer with an oscillator network for entanglement distribution has been demonstrated: superconducting qubits have been used to prepare arbitrary Fock states of a single microwave resonator [11, 6], and a method has been designed to prepare arbitrary entangled states of two resonators [21].

Future Work

Our planned future work on parallel entanglement transfer falls into three categories. First, we hope to verify the conjecture made about parallel entanglement transfer on hypercube spin networks: that if parallel entanglement transfer is performed as in the qubit-compatible protocol, then the fidelity really follows a function form similar to (4.1) (we suspect it is actually given by $F \gtrsim 1 - \frac{1}{2}m\eta^2 \sin^2 \xi_T$). In essence, we hope to justify the name we've given to the qubit-compatible protocol.

Our second goal is to characterize the capacity of other networks—besides the hypercubes—for parallel quantum state transfer. We are especially interested in the completely connected networks, which arise naturally when superconducting qubits are coupled via a microwave resonator.

Finally, we plan to numerically study the effects of disorder and decoherence on parallel quantum state transfer. Parallel quantum state transfer, especially in oscillator networks, inevitably involves higher energy subspaces than single quantum state transfer. Because higher energy states decohere more quickly, this could limit the number states than can be sent at once across a network.

Bibliography

[1] Bose, "Quantum communication through spin chain dynamics: an introductory overview," *arXiv:0802.1224*, 2008.

[2] M. Ansmann, H. Wang, R. C. Bialczak, M. Hofheinz, E. Lucero, M. Neeley, A. D. O'Connell, D. Sank, M. Weides, J. Wenner, A. N. Cleland, and J. M. Martinis, "Violation of bell's inequality in josephson phase qubits," *Nature*, vol. 461, 2009.

[3] M. A. Sillanpää, J. I. Park, and R. W. Simmonds, "Coherent quantum state storage and transfer between two phase qubits via a resonant cavity," *Nature*, vol. 449, 2007.

[4] J. Majer, J. M. Chow, J. M. Gambetta, J. Koch, B. R. Johnson, J. A. Schreier, L. Frunzio, D. I. Schuster, A. A. Houck, A. Wallraff, A. Blais, M. H. Devoret, S. M. Girvin, and R. J. Schoelkopf, "Coupling superconducting qubits via a cavity bus," *Nature*, vol. 449, 2007.

[5] M. Christandl, N. Datta, A. Ekert, and A. J. Landah, "Perfect state transfer in quantum spin networks," *Physical Review Letters*, vol. 92, no. 187902, 2004.

[6] M. Hofheinz, H. Wang, M. Ansmann, R. C. Bialczak, E. Lucero, M. Neeley, A. D. O'Connell, D. Sank, J. Wenner, J. M. Martinis, and A. N. Cleland, "Synthesizing arbitrary quantum states in a superconducting resonator," *Nature*, vol. 459, 2009.

[7] M. A. Nielsen and I. L. Chuang, *Quantum Computation and Quantum Information*. Cambridge University Press, 2002.

[8] F. W. Strauch and C. J. Williams, "Theoretical analysis of perfect quantum state transfer with superconducting phase qubits," *Phys. Rev. B*, vol. 78, p. 094516, 2008.

[9] W. K. Wootters and W. H. Zurek, "A single quantum cannot be cloned," *Nature*, vol. 299, no. 5886, pp. 802,803, 1982.

[10] F. Verstraete, M. Martin-Delgado, and J. I. Cirac, "Diverging entanglement length in gapped quantum spin systems," *Physical Review Letters*, vol. 92, no. 087201, 2004.

[11] M. Hofheinz, E. M. Weig, M. Ansmann, R. C. Bialczak, E. Lucero, M. Neeley, A. D. O'Connell, H. Wang, J. M. Martinis, and A. N. Cleland, "Generation of fock states in a superconducting quantum circuit," *Nature*, vol. 454, 2008.

[12] J. P. Hays and T. Mudge, "Hypercube supercomputers," *Proceedings of the IEEE*, vol. 77, no. 12, 1989.

[13] F. Harary, J. P. Hayes, and H. J. Wu, "A survey of the theory of hypercube graphs," *Computational and Applied Mathematics*, vol. 15, no. 4, 1988.

[14] W. D. Hillis, "Richard Feynman and the Connection Machine," *Physics Today*, vol. 42, 89.

[15] J. Kempe, "Quantum random walks - an introductory overview," *Contemporary Physics*, vol. 44, no. 4, 2003.

[16] F. W. Strauch, "Reexamination of decoherence in quantum walks on the hypercube," *Physical Review A*, vol. 79, no. 032319, 2009.

[17] C. H. Bennett, G. Brassard, C. Crepeau, R. Jozsa, A. Peres, and W. K. Wootters, "Teleporting an unknown quantum state via dual classical and einstein-podolsky-rosen channels," *Physical Review Letters*, vol. 70, 1993.

[18] M. A. Nielsen, "A simple formula for the average gate fidelity of a quantum dynamical operation," *Physics Letters A*, vol. 303, no. 4, pp. 249 – 252, 2002.

[19] C. H. Bennett, G. Brassard, S. Popescu, B. Schumacher, J. A. Smolin, and W. K. Wootters, "Purification of noisy entanglement and faithful teleportation via noisy c1hannels," *Physical Review Letters*, vol. 76, pp. 772–775, 1996.

[20] D. Bruß, "Characterizing entanglement," *Journal of Mathematical Physics*, vol. 43, no. 9, pp. 4237–4251, 2002.

[21] F. W. Strauch, K. Jacobs, and R. W. Simmonds, "Arbitrary control of entanglement between two superconducting resonators," *arXiv:1003.4284*, 2010.

[22] T. J. Osborne, "Statics and dynamics of quantum xy and heisenberg systems on graphs," *Phys. Rev. B*, vol. 74, p. 094411, Sep 2006.

[23] P. W. Shor, J. A. Smolin, and B. M. Terhal, "Nonadditivity of bipartite distillable entanglement follows from a conjecture on bound entangled werner states," *Phys. Rev. Lett.*, vol. 86, pp. 2681–2684, Mar 2001.